Prepared for submission to JCAP

Scalar-tensor theories of gravity, neutrino physics, and the H_0 tension

Mario Ballardini,[a,b,c,d,1] **Matteo Braglia,**[a,b,c] **Fabio Finelli,**[b,c] **Daniela Paoletti,**[b,c] **Alexei A. Starobinsky,**[e,f] **Caterina Umiltà**[g]

[a]Dipartimento di Fisica e Astronomia, Alma Mater Studiorum Università di Bologna, via Gobetti 93/2, I-40129 Bologna, Italy

[b]INAF/OAS Bologna, via Piero Gobetti 101, I-40129 Bologna, Italy

[c]INFN, Sezione di Bologna, via Irnerio 46, I-40126 Bologna, Italy

[d]Department of Physics & Astronomy, University of the Western Cape, Cape Town 7535, South Africa

[e]Landau Institute for Theoretical Physics, 119334 Moscow, Russia

[f]Bogolyubov Laboratory of Theoretical Physics, Joint Institute for Nuclear Research, 141980 Dubna, Moscow Region, Russia

[g]Department of Physics, University of Illinois Urbana-Champaign, Urbana, IL 61801

E-mail: mario.ballardini@inaf.it, matteo.braglia2@unibo.it, fabio.finelli@inaf.it, daniela.paoletti@inaf.it, alstar@landau.ac.ru, umilta@illinois.edu

Abstract. We use *Planck* 2018 data to constrain the simplest models of scalar-tensor theories characterized by a coupling to the Ricci scalar of the type $F(\sigma)R$ with $F(\sigma) = N_{pl}^2 + \xi\sigma^2$. We update our results with previous *Planck* and BAO data releases obtaining the tightest constraints to date on the coupling parameters, that is $\xi < 5.5 \times 10^{-4}$ for $N_{pl} = 0$ (induced gravity or equivalently extended Jordan-Brans-Dicke) and $(N_{pl}\sqrt{8\pi G}) - 1 < 1.8 \times 10^{-5}$ for $\xi = -1/6$ (conformal coupling), both at 95% CL. Because of a modified expansion history after radiation-matter equality compared to the ΛCDM model, all these dynamical models accommodate a higher value for H_0 and therefore alleviate the tension between *Planck*/BAO and distance-ladder measurement from SNe Ia data from 4.4σ at best to 2.7-3.2σ with CMB alone and 3.5-3.6σ including BAO data. We show that all these results are robust to changes in the neutrino physics. In comparison to the ΛCDM model, partial degeneracies between neutrino physics and the coupling to the Ricci scalar allow for smaller values $N_{\rm eff} \sim 2.8$, 1σ lower compared to the standard $N_{\rm eff} = 3.046$, and relax the upper limit on the neutrino mass up to 40%.

[1]Corresponding author.

Contents

1 Introduction

The distance-ladder measurement of the Hubble constant from supernovae type Ia (SNe Ia) [1, 2] and from strong-lensing time delays [3–5] disagrees with the value inferred from the fit of the cosmic microwaves background (CMB) anisotropies [6, 7]. In particular, the value inferred using the *Planck* legacy data for a flat ΛCDM cosmological model, $H_0 = (67.36 \pm 0.54)$ km s^{-1}Mpc^{-1} [7], is in a 4.4σ tension with the most recent measurement from the SH0ES team [8], that is $H_0 = (74.03 \pm 1.42)$ km s^{-1}Mpc^{-1}, determined using Cepheid-calibrated SNe Ia with new parallax measurements from HST spatial scanning [2] and from Gaia DR2 [9], in a 3.2σ tension with the strong-lensing time delay determination from the H0LiCOW collaboration [5], that is $H_0 = \left(73.3^{+1.7}_{-1.8}\right)$ km s^{-1}Mpc^{-1}, and in a 5.3σ tension with the combined SH0ES + H0LiCOW value $H_0 = (73.8 \pm 1.1)$ km s^{-1}Mpc^{-1} [5].

Although it does not seem possible to completely solve the discrepancy between CMB and local measurements by considering unaccounted systematic effects [10–12], revisions of the determination of the Hubble rate based on the Cepheid calibration [13–15], and from SNe Ia calibrated using the tip of the red giant branch method [16] point to values which are still higher than the *Planck* measurements, i.e. ~ 70 km s^{-1}Mpc^{-1}, but to a smaller extent (see however [17–21] for more recent developments).

Alternatively, the H_0 *tension* can be addressed by evoking new physics beyond the ΛCDM concordance model, either in the late or early time Universe [22, 23]. Late-time modifications include a phantom-like dark energy (DE) component [24–26], a vacuum phase transition [27–31], interacting dark energy [32–36], or quintessence in a non-flat Universe [37]. However, these models are tightly constrained [1, 25, 33, 38] by late-time observational data, especially those from baryon acoustic oscillations (BAO) [39–41].

With the highly precisely determined angular scale of the last-scattering surface (LSS) [42], it has been suggested that a smaller value of the comoving sound horizon at baryon drag r_s can provide a higher value of H_0 without spoiling the CMB angular power spectrum measurements and without changing the BAO observables [23, 43]. An example of such an early-time modification is the extension to additional light relics, eventually interacting with hidden dark sectors [44–51]. Another promising early-time solution, is an exotic early dark energy (EDE) component that remains subdominant for the majority of the cosmological evolution of the Universe and injects a small amount of energy in a very narrow redshift window [52–57]. Note that features in the primordial power spectrum [58, 59] and modifications of the recombination history [60, 61] are not able to increase H_0.

Another interesting possibility is to alleviate the H_0 *tension* through a modification of General Relativity (GR) [62–71], which can include early- and late-time modifications of the expansion history with respect to ΛCDM. Scalar-tensor theories of gravity that involve a scalar field non-minimally coupled to the Ricci scalar naturally change the effective relativistic degrees of freedom in the radiation-dominated epoch and the background expansion history from ΛCDM, thus leading to a higher CMB-inferred H_0 [62, 63, 66]. This has been shown for the extended Jordan-Brans-Dicke (eJBD) model in Refs. [62, 63] where the cosmological parameters estimation has been carried out using data from the *Planck* 2013 and 2015 release respectively. The robustness of a higher H_0 in these theories has been proved in Ref. [66], where a more general form of the non-minimal coupling (NMC) to gravity has been considered. In this paper, we confirm earlier results for the particular cases of eJBD and a conformally coupled (CC) scalar field using the most recent cosmological data.

Since the mechanism that drives a higher inferred H_0 relies on the radiation-like behavior of the scalar field at early times, it is interesting to investigate to what extent these simple scalar-tensor theories are degenerate with effective number of relativistic species due to neutrinos and to any additional massless particles produced well before recombination $N_{\rm eff}$. The current tight constraints from the latest *Planck* 2018 data $N_{\rm eff} = 2.89 \pm 0.19$ ($N_{\rm eff} = 2.99 \pm 0.17$ including BAO) at 68% CL [7] can be changed in modified gravity theories as previously shown in the context of $f(R)$ gravity in [72, 73].

While changing $N_{\rm eff}$ can lead to a higher value for H_0 compared with the value inferred in the ΛCDM model from the CMB anisotropies measurements, in the extension of ΛCDM model with non-zero total neutrino mass m_ν, lower values of H_0 correspond to higher values of m_ν and higher values of H_0 correspond to lower m_ν. For instance, the constraint from *Planck* 2018 data in combination with BAO data is $m_\nu < 0.12$ eV at 95% CL [7, 74] and combining with the measurement from the SH0ES team the limit further tightens to $m_\nu < 0.076$ eV [75]. In scalar-tensor theories of gravity, it is possible to keep fixed the angular diameter distance at decoupling or even increase it in order to recover a higher H_0 while increasing the total neutrino mass value [76]. Given that neutrino oscillations are the only laboratory evidence of physics beyond the Standard Model of Particle Physics [77], it is natural to ask ourselves either how the cosmological constraints on neutrino physics can be relaxed in these simple models of scalar-tensor theories compared to the ΛCDM concordance model and how much constraints become larger in the NMC models including the neutrino parameters.

Future CMB experiments, such as the Simons Observatory[1] [78], CMB-S4[2] [79], and future LSS surveys from DESI[3] [80], Euclid[4] [81, 82], LSST[5] [83], SKA[6] [84, 85] will help to improve the constraints on these extended cosmologies [86–88] and limit the degeneracy of neutrino parameters $N_{\rm eff}$ and m_ν with scalar-tensor theories [89].

The paper is organized as follows. Sec. 2 is devoted to a description of the models considered. We describe the datasets considered in Sec. 3. In in Sec. 4, we start by discussing the updated constraints on the eJBD and CC model in light of new CMB and BAO data, then we discuss the combination with the distance-ladder measure of H_0 from SNe Ia in Sec. 5. We further improve the analysis by extending the cosmological parameters to the ones describing the neutrino sector in Secs. 6.1-6.2-6.3. We draw our conclusions in Sec. 7. In App. A, we collect all the tables with the constraints on the cosmological parameters obtained with our MCMC analysis.

2 The model: non-minimally coupled scalar-tensor theory

As far as cosmological tests are concerned, one of workhorse models to test deviations from GR is the eJBD [90, 91] theory, which has been extensively studied [62, 63, 67, 92–97]. NMC eJBD theory is perhaps the simplest extension to GR within the more general Horndeski theory [98]:

$$S = \int \mathrm{d}^4x\sqrt{-g}\left[\frac{F(\sigma)}{2}R - \frac{g^{\mu\nu}}{2}\partial_\mu\sigma\partial_\nu\sigma - V(\sigma) + \mathcal{L}_m\right] , \tag{2.1}$$

where $F(\sigma) = N_{pl}^2 + \xi\sigma^2$, R is the Ricci scalar, and $\mathcal{L}_m$ is the Lagrangian density for matter fields. As in [66], we do not consider a quintessence-like inverse power-law potential (see for instance [99–103]), but we restrict ourselves to a potential of the type $V(\sigma) = \lambda F^2(\sigma)/4$ for which the scalar field is effectively massless. Our choice reduces to eJBD theory after the redefinition $\sigma^2 = \phi/(8\pi\xi)$, $\xi = 1/(4\omega_{\rm BD})$, and setting $N_{pl} = 0$.

For a flat Friedmann-Lemaître-Robertson-Walker (FLRW) Universe with $\mathrm{d}s^2 = -\mathrm{d}t^2 + a^2(t)\mathrm{d}\mathbf{x}^2$, the background Friedmann equations in the Jordan frame are [104]:

$$3FH^2 = \rho_m + \frac{\dot\sigma^2}{2} + V(\sigma) - 3H\dot F\,, \tag{2.2}$$

$$-2F\dot H = \rho_m + \dot\sigma^2 + \ddot F - H\dot F\,. \tag{2.3}$$

These equations are supplemented by the Klein-Gordon equation that governs the evolution of the scalar field:

$$\Box\sigma - V_\sigma + F_\sigma R = 0\,. \tag{2.4}$$

The coupling between gravity and the scalar degree of freedom induces a time varying Newton's gravitational constant G_N, which is given by $G_N = 1/(8\pi F)$. This quantity is usually denoted by the cosmological Newton's gravitational constant, as opposed to the one that is actually measured in laboratory Cavendish-type experiments which is rather given by [104]:

$$G_{\rm eff} = \frac{1}{8\pi F}\frac{2F + 4F_{,\sigma}^2}{2F + 3F_{,\sigma}^2}\,. \tag{2.5}$$

[1] https://simonsobservatory.org/
[2] https://cmb-s4.org/
[3] http://desi.lbl.gov/
[4] http://sci.esa.int/euclid/
[5] http://www.lsst.org/
[6] http://www.skatelescope.org/

Deviations from GR for a theory of gravitation are parameterized by the so called post-Newtonian (PN) expansion of the metric [105]. In such an expansion, the line element can be expressed as:

$$\mathrm{d}s^2 = -(1 + 2\Phi - 2\beta_{\rm PN}\Phi^2)\mathrm{d}t^2 + (1 - 2\gamma_{\rm PN}\Phi)\mathrm{d}\mathbf{x}^2\,, \tag{2.6}$$

where we have retained only the two non-null contributions to the PN expansion in the case of NMC theories, that is [104]

$$\gamma_{\rm PN} = 1 - \frac{F_{,\sigma}^2}{F + 2F_{,\sigma}^2}\,, \qquad \beta_{\rm PN} = 1 + \frac{F F_{,\sigma}}{8F + 12F_{,\sigma}^2}\frac{\mathrm{d}\gamma_{\rm PN}}{\mathrm{d}\sigma}\,. \tag{2.7}$$

Solar-system experiments agree with GR predictions, for which both $\gamma_{\rm PN}$ and $\beta_{\rm PN}$ are identically equal to unity, at a very precise level. Measurements of the perihelion shift of Mercury constrain $\beta_{\rm PN} - 1 = (4.1 \pm 7.8) \times 10^{-5}$ at 68% CL [105] and Shapiro time delay constrains $\gamma_{\rm PN} - 1 = (2.1 \pm 2.3) \times 10^{-5}$ at 68% CL [106].

In this paper we restrict ourselves to two simple models, both of which only contain one extra parameter with respect to the ΛCDM model: induced gravity (IG) described by $N_{pl} = 0$ and $\xi > 0$, and a conformally coupled scalar field (CC) for which $\xi = -1/6$ and the free parameter is $N_{pl} > M_{pl}$. For both models, the effective value of the Newton's gravitational constant G_N decreases with time, whereas the scalar field σ increases for $\xi > 0$, e.g. for IG, and it decreases for $\xi < 0$, e.g. for CC[1]. We have $\gamma_{\rm PN} < 1$ and $\beta_{\rm PN} \leq 1$ for $\xi > 0$ ($\beta_{\rm PN} = 1$ for IG), whereas $\gamma_{\rm PN} < 1$ and $\beta_{\rm PN} > 1$ for $\xi < 0$.

In order to connect the present value of the field $\sigma_0 \equiv \sigma(z = 0)$ to the gravitational constant, we impose the condition $G_{\rm eff}(\sigma_0) = G$, where $G = 6.67 \times 10^{-8}$ cm^3 g^{-1} s^{-2} is the gravitational constant measured in a Cavendish-type experiment. This corresponds to

$$\tilde{\sigma}_0^2 = \frac{1 + 8\xi}{\xi(1 + 6\xi)} \tag{2.8}$$

for IG and

$$\tilde{\sigma}_0^2 = \frac{18\tilde{N}_{pl}^2(\tilde{N}_{pl}^2 - 1)}{1 + 3\tilde{N}_{pl}^2}\,, \tag{2.9}$$

for the CC case. For simplicity, we denote quantities normalized to $M_{pl} \equiv 1/\sqrt{8\pi G}$ with a tilde.

3 Methodology and datasets

In order to derive the constraints on the cosmological parameters we use a Markov Chain Monte Carlo (MCMC) analysis by using the publicly available code `MontePython`[2] [108, 109] connected to our modified version of the code `CLASS`[3] [110, 111], i.e. `CLASSig` [62]. Mean values and uncertainties on the parameters reported, as well as the contours plotted, have been obtained using `GetDist`[4] [112]. We use adiabatic initial conditions for the scalar field perturbations [66, 113].

[1]We refer the interested reader to Refs. [62, 63, 66] for a detailed analysis of the background dynamics in these models, see also Ref. [107] for the generalization to anisotropic homogeneous cosmological models of the Bianchi I type.

[2]https://github.com/brinckmann/montepython_public

[3]https://github.com/lesgourg/class_public

[4]https://getdist.readthedocs.io/en/latest

As baseline, we vary the six cosmological parameters for a flat ΛCDM concordance model, i.e. ω_b, ω_c, H_0, τ, $\ln\left(10^{10}A_s\right)$, n_s, plus one extra parameter related to the coupling to the Ricci curvature. For IG ($N_{pl}=0$, $\xi>0$), we sample on the quantity $\zeta_{\rm IG}\equiv\ln\left(1+4\xi\right)$, according to [62, 63, 96] in the prior range [0, 0.039]. For CC ($N_{pl}>M_{pl}$, $\xi=-1/6$), we sample on $\Delta\tilde{N}_{pl}\equiv\tilde{N}_{pl}-1$, according to [66], with prior range [0, 0.5]. In our updated analysis in Sec. 4 we assume 3 massless neutrino with $N_{\rm eff}=3.046$, but a more general neutrino sector is considered in the rest of the paper.

We quote constraints on the variation of the Newton's gravitational constant between the radiation era and the present time $\delta G_N/G_N$, and its derivative at present time $\dot{G}_N/G_N$. Defining the effective cosmological gravitational strength [95]:

$$\frac{G_N}{G}(z=0)=\frac{1}{F(\sigma_0)}\,, \tag{3.1}$$

we have

$$\frac{\delta G_N}{G_N}(z=0)=\frac{G_N(\sigma_0)-G_N(\sigma_{\rm ini})}{G_N(\sigma_{\rm ini})}=\frac{\sigma_{\rm ini}^2-\sigma_0^2}{\sigma_0^2}\leq 0\,, \tag{3.2}$$

$$\frac{\dot{G}_N}{G_N}(z=0)=-\frac{2\dot{\sigma}_0}{\sigma_0}\leq 0\,, \tag{3.3}$$

$$\frac{G_N}{G}(z=0)=\frac{1+6\xi}{1+8\xi}\leq 1\,, \tag{3.4}$$

for IG and

$$\frac{\delta G_N}{G_N}(z=0)=\xi\frac{\sigma_{\rm ini}^2-\sigma_0^2}{N_{pl}^2+\xi\sigma_0^2}=\frac{\sigma_0^2-\sigma_{\rm ini}^2}{6N_{pl}^2-\sigma_0^2}\leq 0\,, \tag{3.5}$$

$$\frac{\dot{G}_N}{G_N}(z=0)=-\frac{2\xi\dot{\sigma}_0\sigma_0}{N_{pl}^2+\xi\sigma_0^2}=\frac{2\dot{\sigma}_0\sigma_0}{6N_{pl}^2-\sigma_0^2}\leq 0\,, \tag{3.6}$$

$$\frac{G_N}{G}(z=0)=\frac{1}{4}\left(3+\frac{M_{pl}^2}{N_{pl}^2}\right)\leq 1\,, \tag{3.7}$$

for the CC case, where $\delta G_N/G_N$, $\dot{G}_N/G_N=0$ and $G_N/G=1$ correspond to the predictions in GR.

We also list the $\Delta\chi^2\equiv\chi^2-\chi^2_{\Lambda CDM}$, where negative values indicate a better-fit to the datasets with respect to the ΛCDM model.

3.1 Datasets

We constrain the cosmological parameters using several combination of datasets. Our CMB measurements are those from the *Planck* 2018 legacy release (hereafter P18) on temperature, polarization, and weak lensing CMB anisotropies angular power spectra [114, 115]. The high-multipoles likelihood $\ell\geq 30$ is based on `Plik` likelihood. We use the low-ℓ likelihood combination at $2\leq\ell<30$: temperature-only `Commander` likelihood plus the `SimAll` EE-only likelihood. For the *Planck* CMB lensing likelihood, we consider the *conservative* multipoles range, i.e. $8\leq\ell\leq 400$. We marginalize over foreground and calibration nuisance parameters of the *Planck* likelihoods [114, 115] which are also varied together with the cosmological ones.

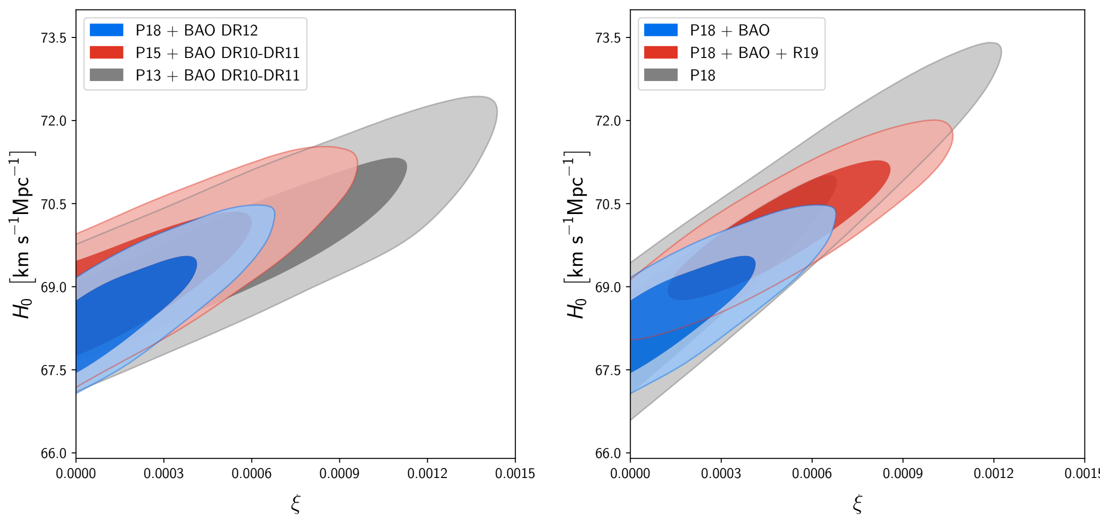

Figure 1. Left panel: marginalized joint 68% and 95% CL regions 2D parameter space using current versus previous releases of *Planck* data and BOSS BAO data from [62, 63]. Right panel: marginalized joint 68% and 95% CL regions 2D parameter space using P18 (gray) in combination with BAO (blue) and BAO + R19 (red) for the IG model.

Baryon acoustic oscillation (BAO) measurements from galaxy redshift surveys are used as primary astrophysical dataset to constraint these class of theories providing a complementary late-time information to the CMB anisotropies. We use the Baryon Spectroscopic Survey (BOSS) DR12 [41] *consensus* results on BAOs in three redshift slices with effective redshifts $z_{\rm eff} = 0.38, 0.51, 0.61$ [116–118], in combination with measure from 6dF [39] at $z_{\rm eff} = 0.106$ and the one from SDSS DR7 [40] at $z_{\rm eff} = 0.15$.

Finally, we consider the combination with a Gaussian likelihood based on the determination of the Hubble constant from from Hubble Space Telescope (HST) observations (hereafter R19), i.e. $H_0 = (74.03 \pm 1.42)$ km s^{-1}Mpc^{-1} [8].

4 Updated *Planck* 2018 results

The results in this section update those obtained in Ref. [63] for IG and in Ref. [66] for CC, based on the *Planck* 2015 data (P15) [119, 120] in combination with an older compilation of BAO data, i.e. DR10-DR11 [39, 40, 122].

First, we discuss the IG case. We find that the constraint on the coupling parameter ξ obtained from the CMB alone is almost half of the bound obtained with P15 which was $\xi < 0.0017$ at 95% CL. With the full high-ℓ polarization information and the new determination of τ we obtain $\xi < 0.00098$ at 95% CL. Adding the BAO data, we obtain $\xi < 0.00055$ at 95% CL, which is 25% tighter compared to the limit obtained with P15 in combination with BAO DR10-11, i.e. $\xi < 0.00075$ and half of the one obtained with P13 in combination with BAO DR10-11, i.e. $\xi < 0.0012$, see the left panel of Fig. 1. As we can see from Tab. 1, BAO data strongly constrain the model and are useful to break the degeneracy in the $H_0 - \xi$ parameter space.

We now discuss the CC case. The coupling to gravity is constrained to $N_{pl} < 1.000028\ \mathrm{M}_{pl}$ at 95% CL for P18 and $N_{pl} < 1.000018\ \mathrm{M}_{pl}$ at 95% CL in combination with BAO data. These constraints update the ones obtained with P15 in combination with D10-DR11 BAO

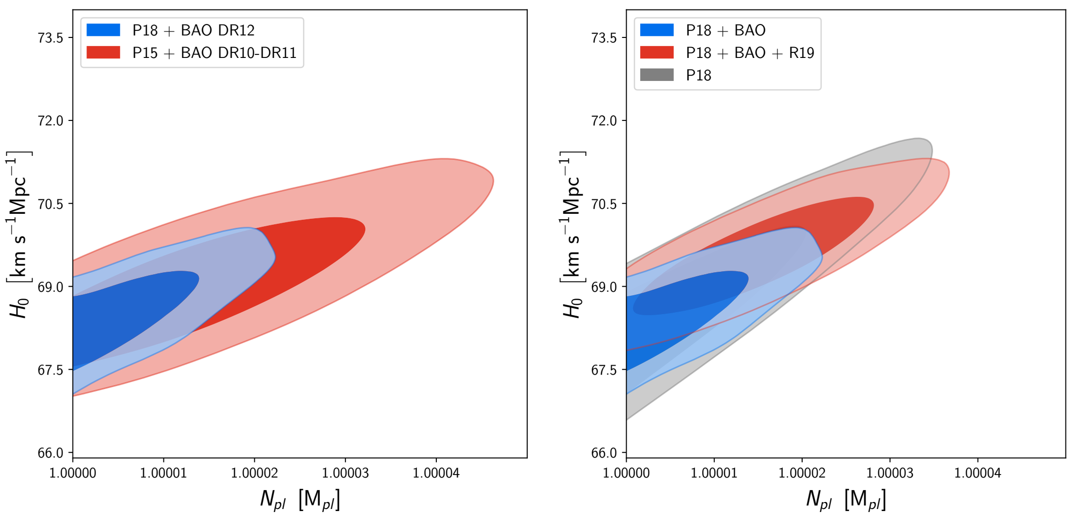

Figure 2. Left panel: marginalized joint 68% and 95% CL regions 2D parameter space using P18 (P15) data in combination BAO in blue (red). Right panel: marginalized joint 68% and 95% CL regions 2D parameter space using P18 (gray) in combination with BAO (blue) and BAO + R19 (red) for the CC model.

$N_{pl} < 1.000038$ M$_{pl}$ at 95% CL in Ref. [66]. As in the IG case, we still have a degeneracy between H_0 and the coupling to gravity N_{pl} as visible from Fig. 2. For these NMC models we recover the same cosmological parameters and uncertainties if we allow ξ to vary, with prior range $[0, 0.1]$ and $[-0.1, 0]$, together with N_{pl}. We find for the positive branch ($N_{pl} < M_{pl}$, $\xi > 0$) of the coupling:

$$N_{pl} > 0.64\ \mathrm{M}_{pl}\ (> 0.60\ \mathrm{M}_{pl})\,, \qquad \xi < 0.046\ (< 0.055) \tag{4.1}$$

both at 95% CL and $H_0 = \left(68.78^{+0.56}_{-0.84}\right)$ km s^{-1}Mpc^{-1} ($70.14^{+0.86}_{-0.72}$ km s^{-1}Mpc^{-1}) with P18+BAO (P18+BAO+R19). The constraints for the negative branch ($N_{pl} > M_{pl}$, $\xi < 0$) are:

$$N_{pl} < 1.05\ \mathrm{M}_{pl}\ (< 1.04\ \mathrm{M}_{pl})\,, \qquad \xi > -0.042\ (> -0.051) \tag{4.2}$$

both at 95% CL and $H_0 = \left(68.76^{+0.54}_{-0.78}\right)$ km s^{-1}Mpc^{-1} (69.74 ± 0.75 km s^{-1}Mpc^{-1}) with P18+BAO (P18+BAO+R19).

Consistently with the constraints on the coupling parameters ξ and N_{pl}, we find also tighter limits on the variation of the Newton's gravitational constant (3.2)-(3.5) and its derivative (3.3)-(3.6) at present time. For IG, we have:

$$\frac{\delta G_{\rm N}}{G_{\rm N}}(z=0) > -0.016\,, \qquad \frac{\dot{G}_{\rm N}}{G_{\rm N}}(z=0) > -0.66 \times 10^{-13}\ \mathrm{yr}^{-1} \tag{4.3}$$

for P18 + BAO at 95% CL, updating those obtained in Ref. [63] with P15 + BAO DR10-11, i.e.

$$\frac{\delta G_{\rm N}}{G_{\rm N}}(z=0) > -0.027\,, \qquad \frac{\dot{G}_{\rm N}}{G_{\rm N}}(z=0) > -1.4 \times 10^{-13}\ \mathrm{yr}^{-1}\,. \tag{4.4}$$

For CC, we obtain the following 95% CL bounds for P18 + BAO:

$$\frac{\delta G_{\rm N}}{G_{\rm N}}(z=0) > -0.017\,, \qquad \frac{\dot{G}_{\rm N}}{G_{\rm N}}(z=0) > -0.25 \times 10^{-23}\ \mathrm{yr}^{-1}\,. \tag{4.5}$$

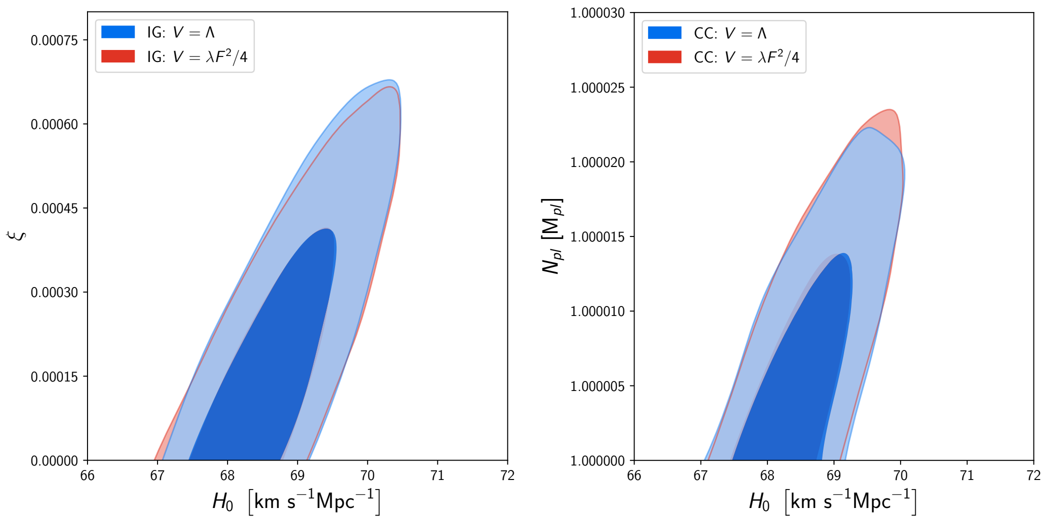

Figure 3. Left panel: marginalized joint 68% and 95% CL regions 2D parameter space $H_0 - \xi$ using P18 + BAO data for IG with $V(\sigma) = \lambda F(\sigma)^2/4$ (red) and $V(\sigma) = \Lambda$ (blue). Right panel: marginalized joint 68% and 95% CL regions 2D parameter space $H_0 - N_{pl}$ using P18 + BAO data for CC with $V(\sigma) = \lambda F(\sigma)^2/4$ (red) and $V(\sigma) = \Lambda$ (blue).

Note that whereas the constraints on $\delta G_{\rm N}/G_{\rm N}(z=0)$ hardly change for different coupling $F(\sigma)$, the limits on $\dot{G}_{\rm N}/G_{\rm N}(z=0)$ strongly depend on the details of the model [1], but are anyway much tighter than those obtained by the Lunar Laser Ranging experiment [121]. Tab. 1 also reports the values of the post-Newtonian parameters as derived parameters from our samples: whereas for IG $\gamma_{\rm PN} \lesssim \mathcal{O}(10^{-3})$, for CC the bounds we derive on $\gamma_{\rm PN}\,, \beta_{\rm PN}$ are now tighter than those in the Solar System.

We note that the value of the initial (final) scalar field is small and sub-Planckian $\sigma_{ini} = (0.22 \pm 0.10)$ M$_{pl}$ ($\sigma_0 = (0.0089 \pm 0.0040)$ M$_{pl}$) as opposed to the IG case where the evolution is super-Planckian.

We have tested that our results are stable when we switch to a flat potential $V(\sigma) = \Lambda$ for both IG and CC. We show in Fig. 3 the consistency of the posterior distributions for H_0, ξ, and N_{pl} with current cosmological data (P18 + BAO). The comparison with $V(\sigma) = \Lambda$ for IG updates the results obtained in [63] with *Planck* 2015 which showed that the cosmological parameters were stable when varying the index n of a power-law potential $V(\sigma) = \lambda\sigma^n/4$ with $n \geq 0$. The stability of the results for the CC case when switching to $V(\sigma) = \Lambda$ is a new result, although, in analogy with what happens in IG, not totally unexpected since our data constrains the deviations $\mathcal{O}(\sigma^2/N_{pl}^2)$ of F^2 from a flat potential. We refer the interested reader to Ref. [71] for an extended analysis of $V(\sigma) = \Lambda$ for $F(\sigma) = M_{pl}^2\,[1 + \xi(\sigma/M_{pl})^n]$ with $n = 2, 4$ with flat priors on $\sigma_{\rm ini}$[2].

[1]The same behaviour of the constraints on the variation of the Newton's constant and its derivative has been observed changing the potential $V(\sigma)$ for IG, see Ref. [63].

[2]See also Ref. [70] for similar finding in NMC scalar-tensor gravity with a coupling $F(\sigma) = M_{pl}^2 + \xi\sigma^2$ in the parameter space range for $\xi < 0$.

5 Implications for the H_0 tension and combination with R19 data

We find a higher value for the Hubble parameter for IG, i.e. $H_0 = \left(69.6^{+0.8}_{-1.7}\right)$ km s^{-1}Mpc^{-1}, and for CC, i.e. $H_0 = \left(69.0^{+0.7}_{-1.2}\right)$ km s^{-1}Mpc^{-1}, compared to the ΛCDM case, i.e. $H_0 = (67.36 \pm 0.54)$ km s^{-1}Mpc^{-1}, for P18.

The addition of BAO drives the value for H_0 to lower values, for IG to $H_0 = \left(68.78^{+0.53}_{-0.78}\right)$ km s^{-1}Mpc^{-1} and for CC to $H_0 = \left(68.62^{+0.47}_{-0.66}\right)$ km s^{-1}Mpc^{-1}. Note however that these values are larger than the corresponding ΛCDM value, i.e. $H_0 = (67.66 \pm 0.42)$ km s^{-1}Mpc^{-1}.

Once we include R19, we obtain $H_0 = (70.1 \pm 0.8)$ km s^{-1}Mpc^{-1} at 68% CL, $\xi = 0.00051^{+0.00043}_{-0.00046}$ at 95% CL for IG, $H_0 = \left(69.64^{+0.65}_{-0.73}\right)$ km s^{-1}Mpc^{-1} at 68% CL, $N_{pl} <$ 1.000031 M$_{pl}$ at 95% CL for CC. Fig. 1 shows how the degeneracy between H_0 and ξ can easily accommodate for larger H_0 value with respect to the ΛCDM concordance model reducing the H_0 *tension* from 4.4σ to 2.7σ (3.2σ) for P18 and 3.5σ (3.6σ) including BAO for IG (CC). The reduction of the tension is due to the combination of having an higher mean and larger uncertainties on H_0 compared to the ΛCDM model. We find that H_0 is about ~ 0.5 km s^{-1}Mpc^{-1} higher in the IG compared to the CC case for every choice of datasets combination.

Note that the models considered in our paper can produce a values of H_0 in complete agreement with the local value of H_0 measured using red giants [16], though not that measured using SNe Ia [8].

6 Degeneracy with the neutrino sector

6.1 Effective number of relativistic degrees of freedom

The presence of extra relativistic degrees of freedom in the Universe increases the expansion rate during the radiation-dominated era and shifts the epoch of matter-radiation equality, the shape of the matter power spectrum, and the history of recombination (see Refs. [123, 124] for a review). The extra radiation is usually parameterized by $\Delta N_{\rm eff} \equiv N_{\rm eff} - 3.046$ which takes into account that neutrino decoupling was not quite complete when e^+e^- annihilation began [125–128].

In the context of the H_0 *tension*, a larger value of $N_{\rm eff}$ can attenuate the discrepancy on the H_0 value and reduce the comoving sound horizon at baryon drag. However, the tension is only reduced ($\sim 2\sigma$) and it appears again when BAO data is included [7, 43].

There is an interplay (negative correlation) between the contribution of extra radiation with respect to the standard ΛCDM scenario from the $N_{\rm eff}$ and from the scalar field coupling[1] which acts as an additional source of radiation in the early Universe. Decreasing the effective number of extra relativistic species to $N_{\rm eff} = 2.846$ we obtain deviations of the CMB anisotropies angular power spectra to the ΛCDM model of the same order of the ones obtained with ξ halved and $N_{\rm eff} = 3.046$, see Fig. 4.

We see that, preferring lower values of $N_{\rm eff}$, the dataset allows for larger values for ξ compared to the case with $N_{\rm eff} = 3.046$ fixed. We go from $\xi < 0.00098$ to $\xi < 0.0019$ at 95% CL with P18 alone and from $\xi < 0.00055$ to $\xi < 0.00078$ once we include BAO, see Tab. 3.

The mean of $N_{\rm eff}$ moves around 1σ toward lower values with respect to the ΛCDM case with a similar error. For IG, we get at 68% CL $N_{\rm eff} = 2.79 \pm 0.20$ for P18 compared to $N_{\rm eff} = 2.89 \pm 0.19$ in ΛCDM and $N_{\rm eff} = 2.85 \pm 0.17$ in combination with BAO compared

[1]See Refs. [72, 73] for an application in the context of $f(R)$ gravity.

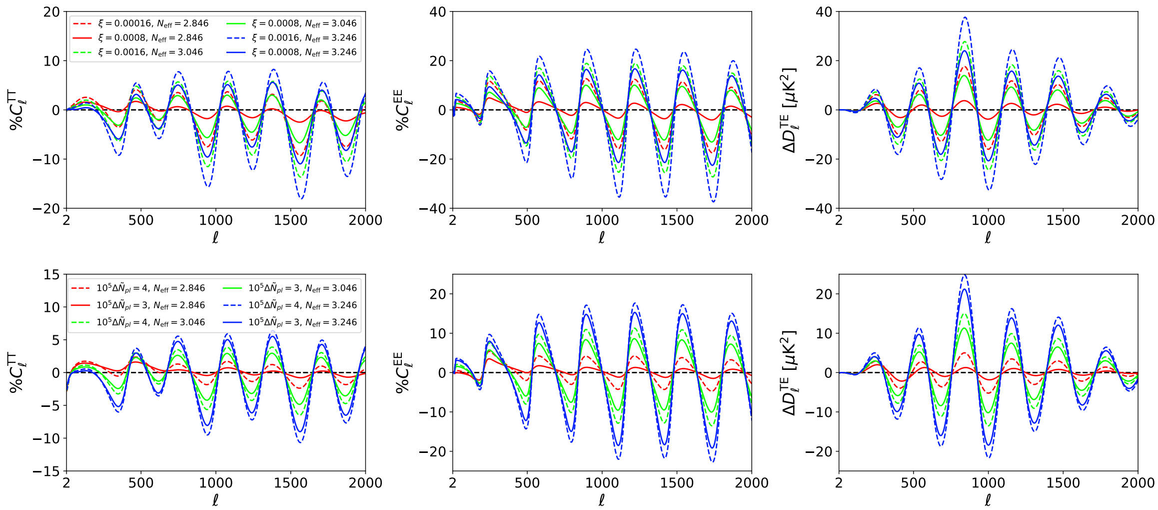

Figure 4. Differences with respect to the ΛCDM with ($N_{\rm eff} = 3.046$) with IG (top panels) for $\xi = 0.0008, 0.0016$ (solid, dashed) and $N_{\rm eff} = 2.846, 3.046, 3.246$ (red, green, blue), and CC (bottom panels) for $N_{pl} = 1.00003, 1.00004$ M_{pl} (solid, dashed) and $N_{\rm eff} = 2.846, 3.046, 3.246$ (red, green, blue). $D_\ell \equiv \ell(\ell+1)C_\ell/(2\pi)$ are the band-power angular power spectra.

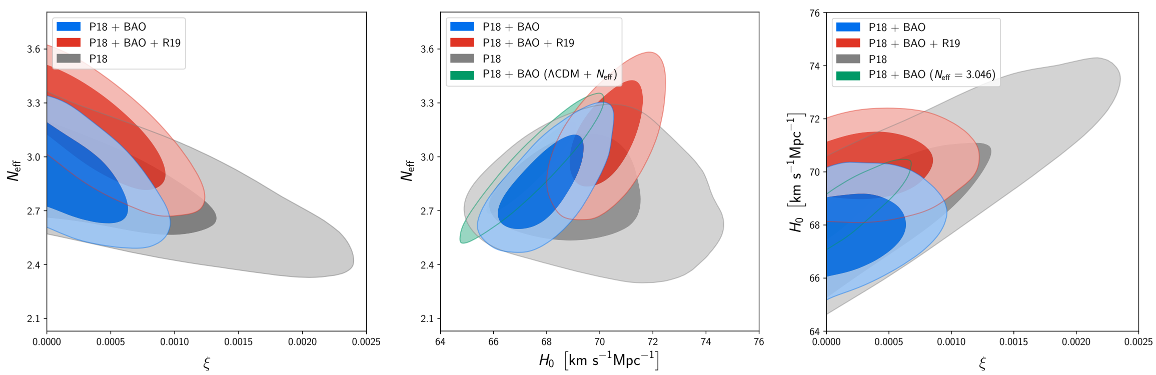

Figure 5. Marginalized joint 68% and 95% CL regions 2D parameter space using the P18 (gray) in combination with BAO (blue) and BAO + R19 (red) for the IG+$N_{\rm eff}$ model. In the central panel, we include the $H_0 - N_{\rm eff}$ contours for the ΛCDM in green. In the right panel, we include the $H_0 - \xi$ contours for the IG with $N_{\rm eff} = 3.046$ in green.

to $N_{\rm eff} = 2.99 \pm 0.17$ in ΛCDM. In Fig. 5 (central panel), we show the enlarged $H_0 - N_{\rm eff}$ parameter space in IG compared to the ΛCDM concordance model (green contours) where it is possible to reach higher value of H_0 without increasing $N_{\rm eff}$ in presence of a modification of gravity.

In the CC model, an analogous correlation in the $N_{\rm eff} - N_{pl}$ parameter space is found, see Fig. 6. The constraints on N_{pl} are larger, from $N_{pl} < 1.000028$ M_{pl} to $N_{pl} < 1.000057$ M_{pl} at 95% CL with P18 alone and from $N_{pl} < 1.000018$ M_{pl} to $N_{pl} < 1.000019$ M_{pl} at 95% CL once we include BAO, see Tab. 4.

While for the combination P18 + BAO we find a higher value for the Hubble parameter for IG, i.e. $H_0 = \left(68.78^{+0.53}_{-0.78}\right)$ km s^{-1}Mpc^{-1}, and for CC, i.e. $H_0 = \left(68.62^{+0.47}_{-0.66}\right)$ km s^{-1}Mpc^{-1}, compared to the ΛCDM+$N_{\rm eff}$ case, i.e. $H_0 = (67.3 \pm 1.1)$ km s^{-1}Mpc^{-1}, the

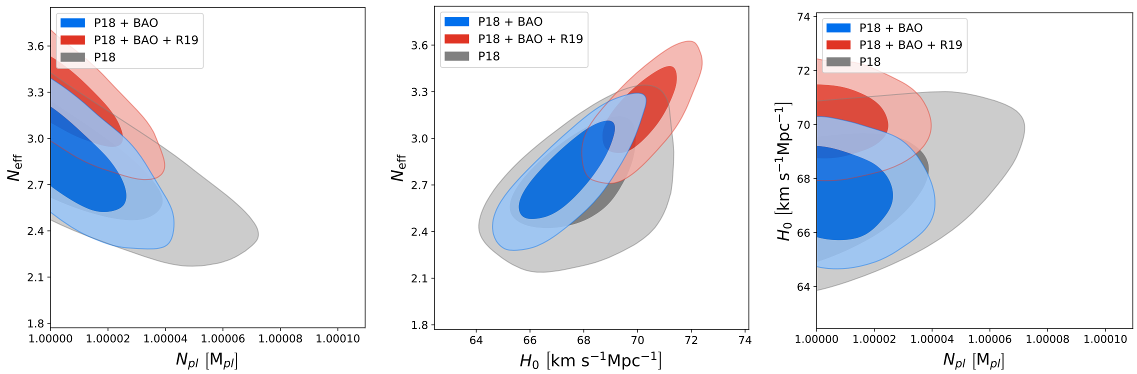

Figure 6. Marginalized joint 68% and 95% CL regions 2D parameter space using the *Planck* legacy data (gray) in combination with DR12 (blue) and DR12 + R19 (red) for the CC+$N_{\rm eff}$ model.

addition of R19 data leads to a closer posterior distribution for H_0 among the three cases, i.e. (70.1 ± 0.8) km s^{-1}Mpc^{-1} for IG, (69.6 ± 0.7) km s^{-1}Mpc^{-1} for CC, and $H_0 = (70.0 \pm 0.9)$ km s^{-1}Mpc^{-1} for ΛCDM+$N_{\rm eff}$. We find a similar posterior distribution also for IG+$N_{\rm eff}$ (CC+$N_{\rm eff}$), i.e. (70.3 ± 0.9) km s^{-1}Mpc^{-1} ((70.1 ± 0.9) km s^{-1}Mpc^{-1}), see Fig. 5.

The addition of BAO data reduces the degeneracy $H_0 - \xi$ $(-N_{pl})$ increasing the one between $N_{\rm eff} - \xi$ $(-N_{pl})$ and $H_0 - N_{\rm eff}$. In order to reduce comoving sound horizon to accommodate a larger value of H_0, in this case $N_{\rm eff}$ is moved towards larger values, i.e. 3.11 ± 0.19 for IG and 3.16 ± 0.19 for CC, see Tab. 3.

6.2 Neutrino mass

The changes in the background evolution caused by neutrino mass, under standard assumptions and for a fixed set of standard cosmological parameters, are confined to late times. In particular, the neutrino mass impact the angular diameter distance and z_Λ (the redshift of matter-to-cosmological-constant equality) (see Refs. [123, 124, 129–133] for a review on neutrino mass in cosmology).

In the standard ΛCDM scenario, a larger value of m_ν results in a lower Hubble rate inferred from the CMB, exacerbating the H_0 *tension*. However, there is partial correlation between the equation of state of dark energy (DE) w and the total neutrino mass m_ν, as first noticed by [130]. When m_ν is increased (or more generally Ω_ν), Ω_m can be kept unchanged, by simultaneously decreasing w, in order to keep the angular diameter distance at decoupling fixed. In this case, the impact of neutrino mass on the background is confined to variations of z_Λ and of the late-time ISW effect.

Cosmological bounds on the neutrino masses can therefore be relaxed by using a DE component rather than a cosmological constant. Vice versa, cosmological constraints on the DE parameters become larger in comparison to cosmologies with massless neutrinos or with the standard minimal assumption of $m_\nu = 0.06$ eV. The same conclusions have been obtained in the context of Galileon gravity [76].

We show in Fig. 7 the combined effect on the CMB anisotropies of varying both ξ and m_ν in the IG model. For a fixed value of the coupling parameter $\xi = 0.0008$, the differences with respect to the ΛCDM concordance model are reduced by increasing the value of the neutrino mass m_ν from 0.1 eV to 0.3 eV. On the late-time observables, i.e. the weak lensing CMB anisotropies and the linear matter power spectrum, the partial degeneracy between

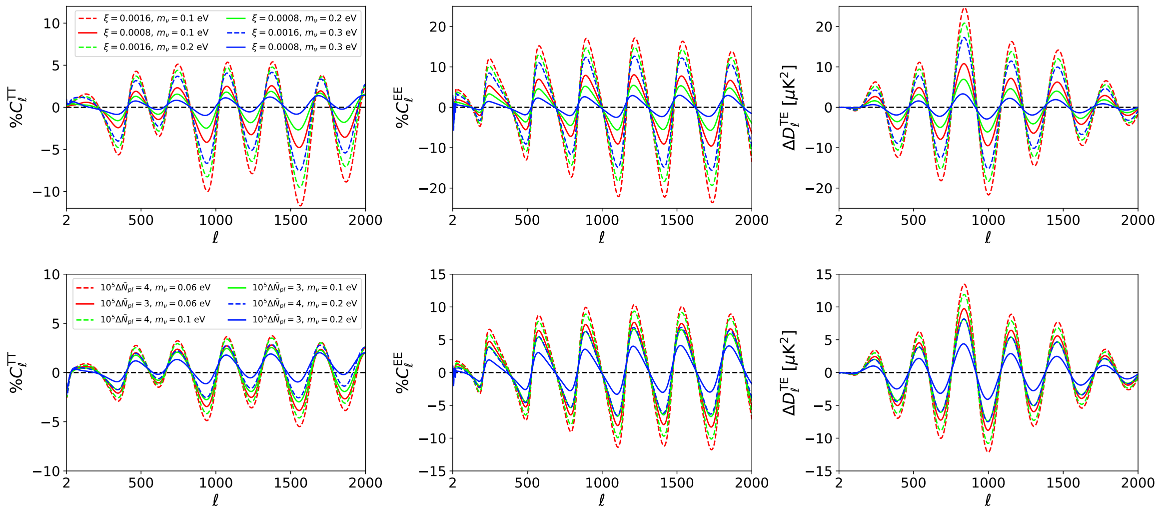

Figure 7. Differences with respect to the ΛCDM with $m_\nu = 0$ eV with IG (top panels) for $\xi = 0.0008, 0.0016$ (solid, dashed) and $m_\nu = 0.1, 0.2, 0.3$ eV (red, green, blue), and CC (bottom panels) for $N_{pl} = 1.00003, 1.00004$ M_{pl} (solid, dashed) and $m_\nu = 0.06, 0.1, 0.2$ eV (red, green, blue).

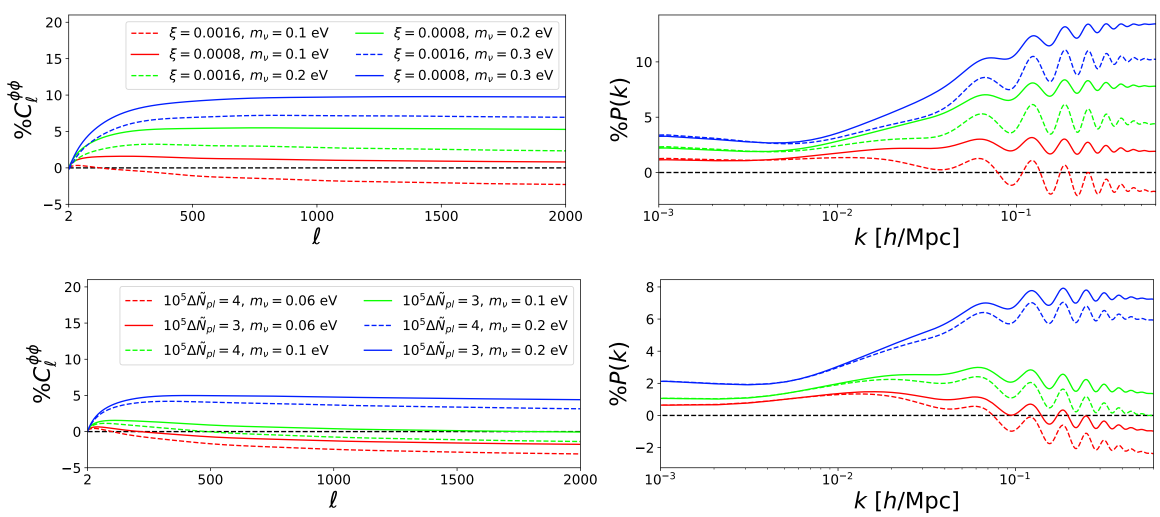

Figure 8. Differences with respect to the ΛCDM with $m_\nu = 0$ eV with IG (top panels) for $\xi = 0.0008, 0.0016$ (solid, dashed) and $m_\nu = 0.1, 0.2, 0.3$ eV (red, green, blue), and CC (bottom panels) for $N_{pl} = 1.00003, 1.00004$ M_{pl} (solid, dashed) and $m_\nu = 0.06, 0.1, 0.2$ eV (red, green, blue).

modified gravity and the neutrino mass is still present but with differences concentrated on small scales, see Fig. 8.

In this case the constraints on the coupling parameter ξ become tighter compared to the case with $m_\nu = 0$, i.e. from $\xi < 0.00098$ to $\xi < 0.00094$ at 95% CL for P18[1]. The CMB anisotropies data prefer to relax the upper bound on the neutrino mass which becomes $m_\nu < 0.31$ eV at 95% CL for P18 29% larger to the ΛCDM case $m_\nu < 0.24$ eV. Including the BAO data, the total neutrino mass is constrained to $m_\nu < 0.17$ eV at 95% CL, 42% larger

[1] We assume one massive and two massless neutrinos.

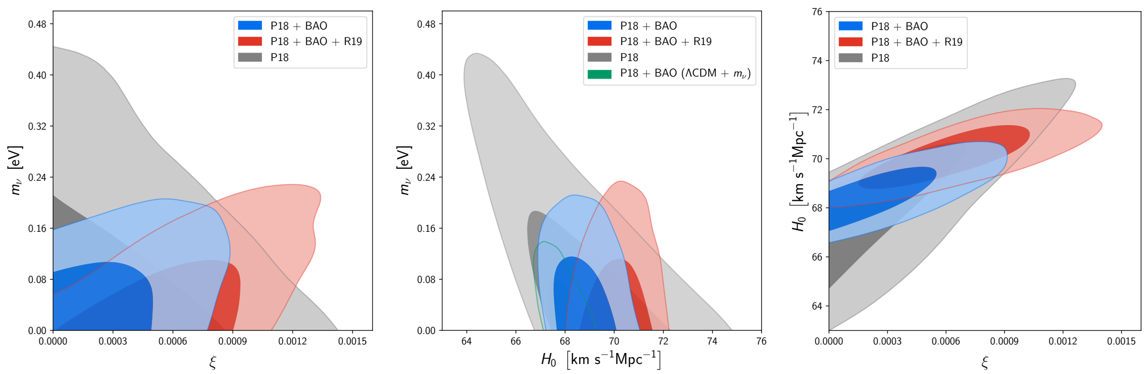

Figure 9. Marginalized joint 68% and 95% CL regions 2D parameter space using P18 (gray) in combination with BAO (blue) and BAO + R19 (red) for the IG+m_ν model. In the central panel, we include the $H_0 - N_{\rm eff}$ contours for the ΛCDM in green.

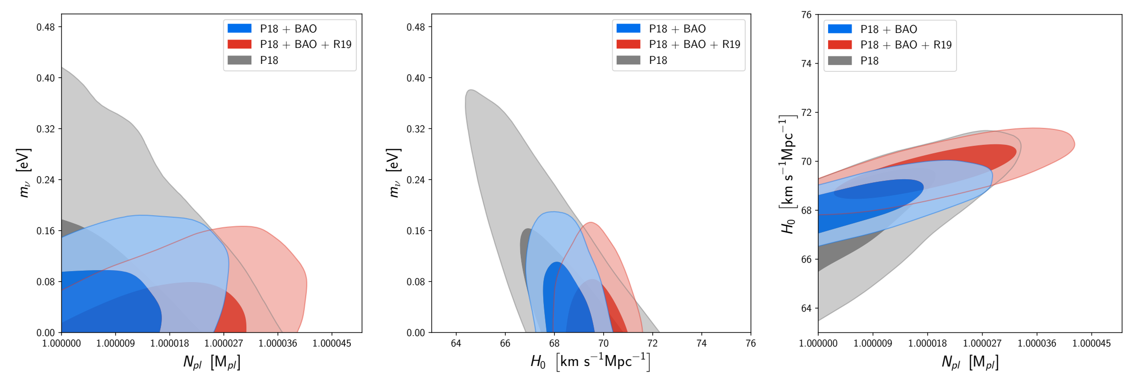

Figure 10. Marginalized joint 68% and 95% CL regions 2D parameter space using P18 (gray) in combination with BAO (blue) and BAO + R19 (red) for the CC+m_ν model.

to the ΛCDM case $m_\nu < 0.12$ eV, and we find $\xi < 0.00076$ at 95% CL, see Tab. 5. The addition of R19 data leads to $H_0 = (70.1 \pm 0.8)$ km s^{-1}Mpc^{-1} with an upper bound on the total neutrino mass $m_\nu < 0.19$ eV at 95% CL, 2.5 times larger than the limit based on the ΛCDM model, with a 2σ detection of the coupling parameter $\xi = 0.00065 \pm 0.00057$ at 95% CL, see Fig. 9.

Analogously, for CC the constraint on N_{pl} becomes tighter compared to the case with $m_\nu = 0$, i.e. $N_{pl} < 1.000026$ M$_{pl}$ for P18 and $N_{pl} < 1.000024$ M$_{pl}$ for P18 + BAO at 95% CL, see Fig. 10. Also, for this model, the upper bound on the neutrino mass becomes 30% larger compared to the ΛCDM case, see Tab. 6.

6.3 Joint constraints on $N_{\rm eff}$ and neutrino mass

Finally, we consider the case where both $N_{\rm eff}$ and m_ν are allowed to vary. Despite the larger parameter space and the larger limits on the parameters, the models do not accommodate higher values of the Hubble parameter compared to the 7- and 8-parameters case analysed before, see Figs. 11-12. Moreover, the total neutrino mass is almost uncorrelated with the Hubble parameter. In this case, the modified gravity parameters ξ and N_{pl} are always compatible at 2σ with the GR limit due to the larger parameter space and are given by (see Tabs. 7-8):

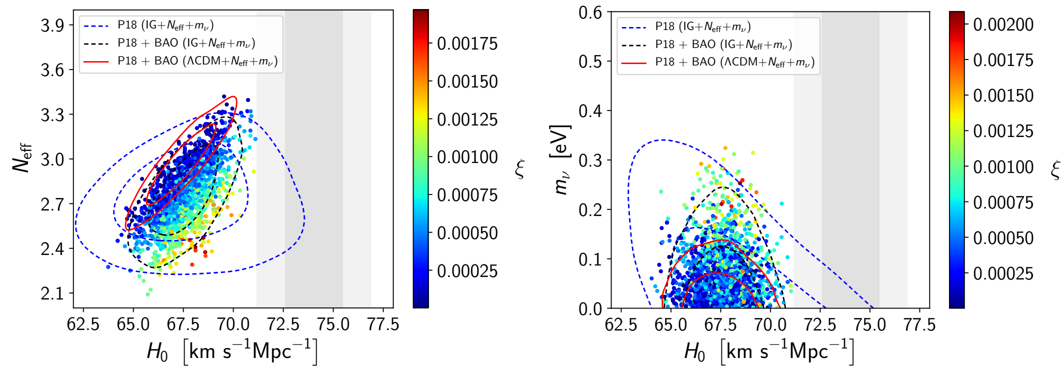

Figure 11. Samples of the P18 + BAO chains in the $H_0 - N_{\rm eff}$ ($H_0 - m_\nu$) plane, colour-coded by ξ for the IG+$N_{\rm eff}$+m_ν model. Dashed blue contours show the constraints for IG+$N_{\rm eff}$+m_ν with P18 alone. Solid red contours show the constraints for the ΛCDM+$N_{\rm eff}$+m_ν model. The gray bands denote the local Hubble parameter measurement from R19 [8].

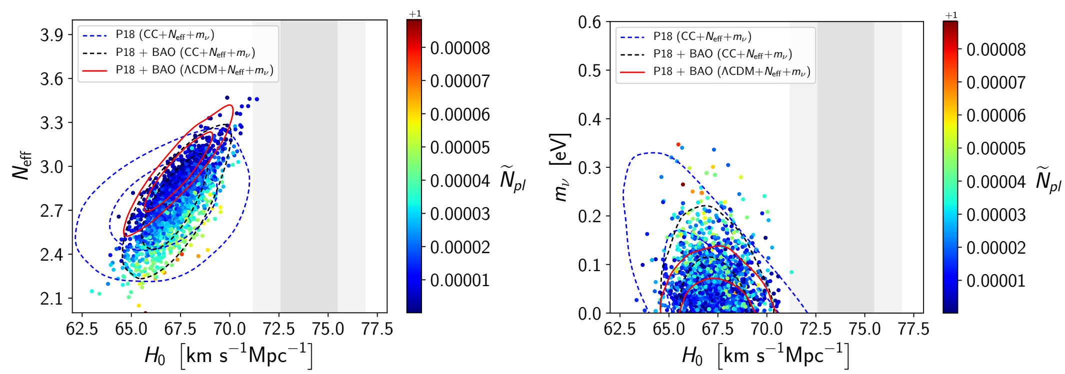

Figure 12. Samples of the P18 + BAO chains in the $H_0 - N_{\rm eff}$ ($H_0 - m_\nu$) plane, colour-coded by N_{pl} for the CC+$N_{\rm eff}$+m_ν model. Dashed blue contours show the constraints for CC+$N_{\rm eff}$+m_ν with P18 alone. Solid red contours show the constraints for the ΛCDM+$N_{\rm eff}$+m_ν model. The gray bands denote the local Hubble parameter measurement from R19 [8].

$$\xi < 0.0018 \text{ (95\% CL)}, \qquad N_{\rm eff} = 2.74 \pm 0.22, \qquad m_\nu < 0.26 \text{ eV (95\% CL)}$$

for IG and

$$N_{pl} < 1.000050 \text{ M}_{pl} \text{ (95\% CL)}, \qquad N_{\rm eff} = 2.73 \pm 0.21, \qquad m_\nu < 0.26 \text{ eV (95\% CL)}$$

for the CC case. When we include BAO data, we obtain

$$\xi < 0.0012 \text{ (95\% CL)}, \qquad N_{\rm eff} = 2.77 \pm 0.20, \qquad m_\nu < 0.19 \text{ eV (95\% CL)}$$

for IG and

$$N_{pl} < 1.000042 \text{ M}_{pl} \text{ (95\% CL)}, \qquad N_{\rm eff} = 2.75 \pm 0.21, \qquad m_\nu < 0.17 \text{ eV (95\% CL)}$$

for the CC case. Adding also R19, we obtain

$$\xi < 0.0013 \text{ (95\% CL)}, \qquad N_{\rm eff} = 3.08 \pm 0.20, \qquad m_\nu < 0.19 \text{ eV (95\% CL)}$$

for IG and

$$N_{pl} < 1.000040 \text{ M}_{pl} \text{ (95\% CL)}\,, \qquad N_{\rm eff} = 3.14 \pm 0.20\,, \qquad m_\nu < 0.14 \text{ eV (95\% CL)}$$

for the CC case.

7 Conclusions

We have studied the simplest class of scalar-tensor theories of gravity where Newton's constant is allowed to vary in time and space. These non-minimally coupled theories are characterized by a coupling to the Ricci scalar R of the type $F(\sigma) = N_{pl}^2 + \xi\sigma^2$, which contain the *induced gravity* [138–140] model for $N_{pl} = 0$ and $\xi > 0$, and the *conformal coupling* model [66] for $\xi = -1/6$. These models contribute to the radiation density budget in the radiation-dominated epoch and change the background expansion history compared to the ΛCDM concordance model naturally alleviating the H_0 *tension*.

Compared to previous constraints [63, 66], the improvement of *Planck* 2018 polarization data lead to tighter results, i.e. $\xi < 0.00098$ and $N_{pl} < 1.000028$ M$_{pl}$ both at 95% CL. When BAO data from BOSS DR12 are added, we obtain tighter limits, i.e. $\xi < 0.00055$ and $N_{pl} < 1.000018$ M$_{pl}$. For $\xi = -1/6$, P18 and BAO data lead to constraints on the post-Newtonian parameters which are tighter than those derived within the Solar System.

It is interesting to note that for CMB and BAO data these models allow for values of H_0 larger than ΛCDM. Using P18 data, we find $H_0 = \left(69.6^{+0.8}_{-1.7}\right)$ km s^{-1}Mpc^{-1} ($H_0 = \left(69.0^{+0.7}_{-1.2}\right)$ km s^{-1}Mpc^{-1}) for the IG (CC) case compared to $H_0 = (67.36 \pm 0.54)$ km s^{-1}Mpc^{-1} for ΛCDM, alleviating the tension from 4.4σ to 2.7σ (3.2σ) for P18 and 3.5σ (3.6σ) including BAO for IG (CC).

Including BAO and R19, we obtain $H_0 = (70.06 \pm 0.81)$ km s^{-1}Mpc^{-1} ($H_0 = \left(69.64^{+0.65}_{-0.73}\right)$ km s^{-1}Mpc^{-1}) for IG (for CC). The value for H_0 we find is similar to what can be obtained in other models which aim to solve the H_0 tension, but the models considered here have just one extra parameter as ΛCDM+$N_{\rm eff}$. Similar valus of H_0 can also be found for NMC beyond the IG and CC cases considered here [71].

We have extended our analysis to a general neutrino sector by allowing the effective number of relativistic species $N_{\rm eff}$ and the neutrino mass m_ν to vary. Both $N_{\rm eff}$ and m_ν are partially degenerate with the deviations from GR, as happens in other modified gravity models [72, 73, 76]. Whereas $N_{\rm eff}$ and the scalar field act as an additional source of radiation in the early Universe, at late times the background contribution to Ω_m due to m_ν can be compensated from the scalar field in order to keep the angular diameter distance at decoupling fixed, see Figs. 4-7-8. We have shown however that these are only partial degeneracies which could be broken by combination of observations at different redshifts.

In case with $N_{\rm eff}$ (Sec. 6.1) the limit on ξ becomes $\sim 94\%$ ($\sim 42\%$) larger with P18 (P18+BAO) while the mean on the number of neutrinos moves around 1σ towards lower values compared to the ΛCDM case without significantly degrading its uncertainty, i.e. $N_{\rm eff} = 2.79 \pm 0.20$ ($N_{\rm eff} = 2.85 \pm 0.17$). For CC the limit on N_{pl} becomes $\sim 104\%$ ($\sim 6\%$) larger with P18 (P18+BAO) and analogously to IG we find $N_{\rm eff} = 2.73^{+0.25}_{-0.22}$ ($N_{\rm eff} = 2.81 \pm 0.19$).

The upper bound on the neutrino mass (Sec. 6.2) is $\sim 29\%$ ($\sim 42\%$) is also degraded with P18 (P18+BAO) compared to the ΛCDM case, i.e. $m_\nu < 0.31$ eV ($m_\nu < 0.17$ eV), whereas the constraint on ξ is slightly tighter with CMB data alone in order to relax the constraint on m_ν. Analogously, for CC the limit on the neutrino mass is $\sim 17\%$ ($\sim 33\%$) larger with P18 (P18+BAO) compared to the ΛCDM case. When both $N_{\rm eff}$ and m_ν are allowed to vary, we see that the constraints on ξ and $N_{\rm pl}$ degrade by a factor two compared to the case with $N_{\rm eff} = 3.046$ and $m_\nu = 0$ eV also in presence of BAO data, i.e. $\xi < 0.0012$ and $N_{pl} < 1.000042$ M$_{pl}$ at 95% CL. For the data used, the combination of the modification to gravity in our models to non-standard neutrino physics does not lead to higher values of H_0 compared to the case with standard assumptions in the neutrino sector.

Acknowledgments

We wish to thank Maria Archidiacono and Thejs Brinckmann for useful suggestions on the use of `MontePython`. MBa, MBr, FF, DP acknowledge financial contribution from the contract ASI/INAF for the Euclid mission n.2018-23-HH.0. FF and DP acknowledge financial support by ASI Grant 2016-24-H.0. AAS was partially supported by the Russian Foundation for Basic Research grant No. 20-02-00411.

A Tables

A.1 Updated *Planck* 2018 results

	P18	P18 + BAO	P18 + BAO + R19
$\omega_{\rm b}$	$0.02244^{+0.00014}_{-0.00016}$	0.02239 ± 0.00013	0.02246 ± 0.00013
$\omega_{\rm c}$	0.1198 ± 0.0012	0.1201 ± 0.0011	0.1200 ± 0.0011
H_0 [km s^{-1}Mpc^{-1}]	$69.6^{+0.8}_{-1.7}$ (2.7σ)	$68.78^{+0.53}_{-0.78}$ (3.5σ)	70.06 ± 0.81 (2.4σ)
τ	$0.0551^{+0.0065}_{-0.0078}$	$0.0545^{+0.0063}_{-0.0071}$	$0.0554^{+0.0064}_{-0.0073}$
$\ln\left(10^{10} A_{\rm s}\right)$	$3.047^{+0.014}_{-0.015}$	3.046 ± 0.013	3.049 ± 0.013
$n_{\rm s}$	$0.9680^{+0.0044}_{-0.0052}$	0.9662 ± 0.0038	0.9688 ± 0.0037
$\zeta_{\rm IG}$	< 0.0039 (95% CL)	< 0.0022 (95% CL)	$0.00202^{+0.00090}_{-0.00100}$
ξ	< 0.00098 (95% CL)	< 0.00055 (95% CL)	$0.00051^{+0.00043}_{-0.00046}$ (95% CL)
γ_{PN}	> 0.9961 (95% CL)	> 0.9978 (95% CL)	$0.9980^{+0.0010}_{-0.0009}$
$\delta G_{\rm N}/G_{\rm N}$ (z=0)	> -0.029 (95% CL)	> -0.016 (95% CL)	-0.0149 ± 0.0068
$10^{13}\dot{G}_{\rm N}/G_{\rm N}$ (z=0) [yr^{-1}]	> -1.16 (95% CL)	> -0.66 (95% CL)	-0.61 ± 0.28
$G_{\rm N}/G$ (z=0)	> 0.9981 (95% CL)	> 0.9989 (95% CL)	$0.99899^{+0.00050}_{-0.00045}$
$\Omega_{\rm m}$	$0.2940^{+0.0150}_{-0.0095}$	$0.3013^{+0.0072}_{-0.0062}$	0.2903 ± 0.0068
σ_8	$0.8347^{+0.0074}_{-0.0130}$	$0.8308^{+0.0067}_{-0.0096}$	0.840 ± 0.010
r_s [Mpc]	$146.37^{+0.79}_{-0.40}$	$146.63^{+0.55}_{-0.34}$	$146.03^{+0.67}_{-0.59}$
$\Delta\chi^2$	0.2	0.2	-3.1

Table 1. Constraints on main and derived parameters (at 68% CL if not otherwise stated) considering P18 in combination with BAO and BAO + R19 for the IG model.

	P18	P18 + BAO	P18 + BAO + R19
$\omega_{\rm b}$	0.02244 ± 0.00015	0.02241 ± 0.00013	0.0250 ± 0.0013
$\omega_{\rm c}$	0.1197 ± 0.0012	0.11990 ± 0.00094	0.1195 ± 0.0010
H_0 [km s^{-1}Mpc^{-1}]	$69.0^{+0.7}_{-1.2}$ (3.2σ)	$68.62^{+0.47}_{-0.66}$ (3.6σ)	$69.64^{+0.65}_{-0.73}$ (2.8σ)
τ	$0.0554^{+0.0064}_{-0.0081}$	$0.0551^{+0.0058}_{-0.0076}$	$0.0562^{+0.0066}_{-0.0077}$
$\ln\left(10^{10} A_{\rm s}\right)$	$3.048^{+0.013}_{-0.016}$	$3.047^{+0.011}_{-0.015}$	$3.050^{+0.013}_{-0.015}$
$n_{\rm s}$	0.9684 ± 0.0047	0.9668 ± 0.0039	0.9707 ± 0.0040
$N_{\rm pl}$ [M$_{\rm pl}$]	< 1.000028 (95% CL)	< 1.000018 (95% CL)	< 1.000031 (95% CL)
γ_{PN}	> 0.999972 (95% CL)	> 0.999982 (95% CL)	> 0.999969 (95% CL)
β_{PN}	< 1.0000023 (95% CL)	< 1.0000015 (95% CL)	< 1.0000025 (95% CL)
$\delta G_{\rm N}/G_{\rm N}$ (z=0)	> -0.026 (95% CL)	> -0.017 (95% CL)	> -0.029 (95% CL)
$10^{13}\dot{G}_{\rm N}/G_{\rm N}$ (z=0) [yr^{-1}]	$> -3.8 \times 10^{-9}$ (95% CL)	$> -2.5 \times 10^{-9}$ (95% CL)	$> -4.2 \times 10^{-9}$ (95% CL)
$G_{\rm N}/G$ (z=0)	> 0.999986 (95% CL)	> 0.999991 (95% CL)	> 0.999985 (95% CL)
$\Omega_{\rm m}$	$0.299^{+0.011}_{-0.009}$	0.3023 ± 0.0061	0.2928 ± 0.0064
σ_8	$0.832^{+0.011}_{-0.007}$	$0.8299^{+0.0060}_{-0.0088}$	$0.8364^{+0.0089}_{-0.011}$
r_s [Mpc]	$146.71^{+0.46}_{-0.33}$	$146.82^{+0.37}_{-0.28}$	$146.53^{+0.51}_{-0.42}$
$\Delta\chi^2$	2.2	0.8	-1.7

Table 2. Constraints on main and derived parameters (at 68% CL if not otherwise stated) considering P18 in combination with BAO and BAO + R19 for the CC model.

A.2 Degeneracy with the neutrino sector: $N_{\rm eff}$

	P18	P18 + BAO	P18 + BAO + R19
$\omega_{\rm b}$	$0.02227^{+0.00018}_{-0.00021}$	0.02225 ± 0.00019	0.02250 ± 0.00019
$\omega_{\rm c}$	0.1161 ± 0.0031	0.1172 ± 0.0030	0.1210 ± 0.0029
H_0 [km s^{-1}Mpc^{-1}]	$69.2^{+1.5}_{-2.4}$ (2.3σ)	$67.9^{+1.0}_{-1.2}$ (3.5σ)	70.28 ± 0.92 (2.2σ)
τ	0.0547 ± 0.0078	0.0526 ± 0.0069	0.0549 ± 0.0072
$\ln\left(10^{10}A_{\rm s}\right)$	3.038 ± 0.016	3.035 ± 0.015	3.050 ± 0.016
$n_{\rm s}$	$0.9617^{+0.0049}_{-0.0088}$	$0.9600^{+0.0045}_{-0.0079}$	0.9707 ± 0.0069
$\zeta_{\rm IG}$	< 0.0076 (95% CL)	< 0.0031 (95% CL)	< 0.0040 (95% CL)
$N_{\rm eff}$	2.79 ± 0.20	2.85 ± 0.17	3.11 ± 0.19
ξ	< 0.0019 (95% CL)	< 0.00078 (95% CL)	< 0.0010 (95% CL)
γ_{PN}	> 0.9925 (95% CL)	> 0.9969 (95% CL)	> 0.9960 (95% CL)
$\delta G_{\rm N}/G_{\rm N}$ (z=0)	> -0.055 (95% CL)	> -0.023 (95% CL)	> -0.029 (95% CL)
$10^{13}\dot{G}_{\rm N}/G_{\rm N}$ (z=0) [yr^{-1}]	> -2.2 (95% CL)	> -0.93 (95% CL)	> -1.2 (95% CL)
$\delta G_{\rm N}/G$ (z=0)	> 0.9962 (95% CL)	> 0.9985 (95% CL)	> -0.9980 (95% CL)
$\Omega_{\rm m}$	$0.290^{+0.022}_{-0.012}$	0.3022 ± 0.0074	0.2906 ± 0.0067
σ_8	$0.834^{+0.012}_{-0.018}$	0.825 ± 0.010	0.841 ± 0.010
r_s [Mpc]	$148.2^{+1.8}_{-1.5}$	148.4 ± 1.7	145.5 ± 1.5
$\Delta\chi^2$	1.7	-1.8	-3.0

Table 3. Constraints on main and derived parameters (at 68% CL if not otherwise stated) considering P18 in combination with BAO and BAO + R19 for the IG+$N_{\rm eff}$ model.

	P18	P18 + BAO	P18 + BAO + R19
$\omega_{\rm b}$	0.02223 ± 0.00022	0.02215 ± 0.00022	0.02257 ± 0.00018
$\omega_{\rm c}$	0.1151 ± 0.0033	0.1162 ± 0.0031	0.1213 ± 0.0030
H_0 [km s^{-1}Mpc^{-1}]	67.9 ± 1.4 (3.1σ)	67.1 ± 1.2 (3.7σ)	70.10 ± 0.92 (2.0σ)
τ	$0.0539^{+0.0060}_{-0.0074}$	$0.0544^{+0.0061}_{-0.0074}$	$0.0561^{+0.0063}_{-0.0075}$
$\ln\left(10^{10}A_{\rm s}\right)$	3.034 ± 0.017	3.035 ± 0.016	$3.053^{+0.014}_{-0.016}$
$n_{\rm s}$	0.9598 ± 0.0084	0.9606 ± 0.0071	0.9736 ± 0.0062
$N_{\rm pl}$ [$\rm M_{pl}$]	< 1.000057 (95% CL)	< 1.000019 (95% CL)	< 1.000032 (95% CL)
$N_{\rm eff}$	$2.73^{+0.25}_{-0.22}$	2.81 ± 0.19	3.16 ± 0.19
γ_{PN}	> 0.999943 (95% CL)	> 0.999981 (95% CL)	> 0.999968 (95% CL)
β_{PN}	< 1.0000048 (95% CL)	< 1.0000015 (95% CL)	< 1.0000027 (95% CL)
$\delta G_{\rm N}/G_{\rm N}$ (z=0)	> -0.052 (95% CL)	> -0.018 (95% CL)	> -0.030 (95% CL)
$10^{13}\dot{G}_{\rm N}/G_{\rm N}$ (z=0) [yr^{-1}]	$> -7.5 \times 10^{-9}$ (95% CL)	$> -2.5 \times 10^{-9}$ (95% CL)	$> -4.3 \times 10^{-9}$ (95% CL)
$G_{\rm N}/G$ (z=0)	> 0.999975 (95% CL)	> 0.999991 (95% CL)	> 0.999984 (95% CL)
$\Omega_{\rm m}$	$0.299^{+0.014}_{-0.011}$	0.3070 ± 0.0066	0.2929 ± 0.0062
σ_8	$0.827^{+0.011}_{-0.013}$	0.8204 ± 0.0099	0.8391 ± 0.0095
r_s [Mpc]	149.5 ± 2.0	149.3 ± 2.0	145.5 ± 1.6
$\Delta\chi^2$	1.4	-0.2	-3.8

Table 4. Constraints on main and derived parameters (at 68% CL if not otherwise stated) considering P18 in combination with BAO and BAO + R19 for the CC+$N_{\rm eff}$ model.

A.3 Degeneracy with the neutrino sector: m_ν

	P18	P18 + BAO	P18 + BAO + R19
$\omega_{\rm b}$	0.02239 ± 0.00017	0.02241 ± 0.00014	0.02247 ± 0.00013
$\omega_{\rm c}$	0.1205 ± 0.0013	0.1203 ± 0.0011	0.1203 ± 0.0012
H_0 [km s^{-1}Mpc^{-1}]	68.5 ± 1.8 (2.4σ)	$68.66^{+0.69}_{-0.87}$ (3.4σ)	70.12 ± 0.81 (2.4σ)
τ	$0.0567^{+0.0065}_{-0.0082}$	$0.0564^{+0.0066}_{-0.0080}$	$0.0572^{+0.0063}_{-0.0080}$
$\ln\left(10^{10}A_{\rm s}\right)$	$3.052^{-0.016}_{+0.013}$	$3.051^{-0.016}_{+0.013}$	$3.054^{+0.013}_{-0.016}$
$n_{\rm s}$	0.9668 ± 0.0053	0.9672 ± 0.0038	0.9700 ± 0.0038
$\zeta_{\rm IG}$	< 0.0037 (95% CL)	< 0.0030 (95% CL)	$0.0026^{+0.0010}_{-0.0013}$
m_ν [eV]	< 0.31 (95% CL)	< 0.17 (95% CL)	< 0.19 (95% CL)
ξ	< 0.00094 (95% CL)	< 0.00076 (95% CL)	0.00065 ± 0.00057 (95% CL)
γ_{PN}	> 0.9963 (95% CL)	> 0.9970 (95% CL)	$0.9974^{+0.0013}_{-0.0010}$
$\delta G_{\rm N}/G_{\rm N}$ (z=0)	> -0.027 (95% CL)	> -0.022 (95% CL)	$-0.0190^{+0.0093}_{-0.0075}$
$10^{13}\dot{G}_{\rm N}/G_{\rm N}$ (z=0) [yr^{-1}]	> -1.1 (95% CL)	> -0.93 (95% CL)	$-0.78^{+0.39}_{-0.31}$
$G_{\rm N}/G$ (z=0)	> 0.9981 (95% CL)	> 0.9985 (95% CL)	$0.9987^{+0.00064}_{-0.00051}$
$\Omega_{\rm m}$	$0.306^{+0.015}_{-0.018}$	0.3029 ± 0.0076	0.2905 ± 0.0068
σ_8	$0.815^{+0.025}_{-0.014}$	$0.821^{+0.014}_{-0.010}$	0.832 ± 0.013
r_s [Mpc]	$146.18^{+0.78}_{-0.38}$	$146.31^{+0.71}_{-0.37}$	$145.56^{+0.78}_{-0.69}$
$\Delta\chi^2$	3.0	0.2	-3.3

Table 5. Constraints on main and derived parameters (at 68% CL if not otherwise stated) considering P18 in combination with BAO and BAO + R19 for the IG+m_ν model.

	P18	P18 + BAO	P18 + BAO + R19
$\omega_{\rm b}$	0.02240 ± 0.00016	0.02242 ± 0.00013	0.02252 ± 0.00013
$\omega_{\rm c}$	0.1203 ± 0.0013	0.12011 ± 0.00097	0.1197 ± 0.0010
H_0 [km s^{-1}Mpc^{-1}]	68.0 ± 1.4 (3.0σ)	$68.31^{+0.62}_{-0.69}$ (3.7σ)	69.62 0.71 (2.8σ)
τ	$0.0563^{+0.0063}_{-0.0080}$	$0.0564^{+0.0065}_{-0.0077}$	$0.0576^{+0.0067}_{-0.0077}$
$\ln\left(10^{10}A_{\rm s}\right)$	$3.051^{+0.013}_{-0.016}$	$3.047^{+0.013}_{-0.015}$	$3.054^{+0.013}_{-0.016}$
$n_{\rm s}$	0.9674 ± 0.0053	0.9681 ± 0.0043	0.9720 ± 0.0041
$N_{\rm pl}$ [M$_{\rm pl}$]	< 1.000026 (95% CL)	< 1.000024 (95% CL)	$1.000019^{+0.000017}_{-0.000018}$ (95% CL)
m_ν [eV]	< 0.28 (95% CL)	< 0.16 (95% CL)	< 0.13 (95% CL)
γ_{PN}	> 0.999926 (95% CL)	> 0.999924 (95% CL)	$0.9999192^{+0.000009}_{-0.000011}$ (95% CL)
β_{PN}	< 1.0000021 (95% CL)	< 1.0000020 (95% CL)	< 1.0000030 (95% CL)
$\delta G_{\rm N}/G_{\rm N}$	> -0.024 (95% CL)	> -0.023 (95% CL)	$-0.0181^{+0.0099}_{-0.0082}$
$10^{13}\dot{G}_{\rm N}/G_{\rm N}$ (z=0) [yr^{-1}]	$> -3.6 \times 10^{-9}$ (95% CL)	$> -3.3 \times 10^{-9}$ (95% CL)	$(-2.7^{+1.5}_{-1.2}) \times 10^{-9}$
$G_{\rm N}/G$ (z=0)	> 0.999987 (95% CL)	> 0.9999988 (95% CL)	$0.9999904^{+0.0000054}_{-0.0000043}$
$\Omega_{\rm m}$	$0.309^{+0.011}_{-0.015}$	0.3047 ± 0.0067	0.2935 ± 0.0064
σ_8	0.814 ± 0.010	$0.820^{+0.013}_{-0.010}$	0.831 ± 0.012
r_s [Mpc]	$146.52^{+0.47}_{-0.34}$	$146.58^{+0.47}_{-0.31}$	$146.26^{+0.55}_{-0.48}$
$\Delta\chi^2$	3.0	0.0	-1.5

Table 6. Constraints on main and derived parameters (at 68% CL if not otherwise stated) considering P18 in combination with BAO and BAO + R19 for the CC+m_ν model.

A.4 Degeneracy with the neutrino sector: ($N_{\rm eff},\ m_\nu$)

	P18	P18 + BAO	P18 + BAO + R19
$\omega_{\rm b}$	0.02218 ± 0.00022	$0.02220^{+0.00022}_{-0.00019}$	0.02250 ± 0.00020
$\omega_{\rm c}$	0.1162 ± 0.0034	0.1164 ± 0.0031	0.1208 ± 0.0030
H_0 [km s^{-1}Mpc^{-1}]	$67.7^{+2.0}_{-2.4}$ (2.6σ)	$67.6 \pm 1.2 (3.5\sigma)$	70.25 ± 0.92 (2.2σ)
τ	$0.0556^{+0.0065}_{-0.0083}$	$0.0554^{+0.0065}_{-0.0073}$	$0.0576^{+0.0063}_{-0.0081}$
$\ln\left(10^{10}A_{\rm s}\right)$	$3.039^{-0.018}_{+0.016}$	3.039 ± 0.016	3.056 ± 0.016
$n_{\rm s}$	0.9577 ± 0.0086	0.9582 ± 0.0076	0.9710 ± 0.0071
$\zeta_{\rm IG}$	< 0.0070 (95% CL)	< 0.0047 (95% CL)	< 0.0053 (95% CL)
m_ν [eV]	< 0.26 (95% CL)	< 0.19 (95% CL)	< 0.19 (95% CL)
$N_{\rm eff}$	2.74 ± 0.22	2.77 ± 0.20	3.08 ± 0.20
ξ	< 0.0018 (95% CL)	< 0.0012 (95% CL)	< 0.0013 (95% CL)
γ_{PN}	> 0.9931 (95% CL)	> 0.9954 (95% CL)	> 0.9948 (95% CL)
$\delta G_{\rm N}/G_{\rm N}$ (z=0)	> -0.050 (95% CL)	> -0.034 (95% CL)	> -0.038 (95% CL)
$10^{13}\dot{G}_{\rm N}/G_{\rm N}$ (z=0) [yr^{-1}]	> -2.0 (95% CL)	> -1.4 (95% CL)	> 1.6 (95% CL)
$G_{\rm N}/G$ (z=0)	> 0.9966 (95% CL)	> 0.9977 (95% CL)	> 0.9974 (95% CL)
$\Omega_{\rm m}$	$0.303^{+0.022}_{-0.019}$	0.3035 ± 0.0081	0.2904 ± 0.0069
σ_8	$0.814^{+0.025}_{-0.019}$	$0.815^{+0.015}_{-0.012}$	$0.833^{+0.013}_{-0.011}$
r_s [Mpc]	148.6 ± 1.9	148.6 ± 1.8	145.3 ± 1.6
$\Delta\chi^2$	1.1	0.5	−2.5

Table 7. Constraints on main and derived parameters (at 68% CL if not otherwise stated) considering P18 in combination with BAO and BAO + R19 for the IG+$N_{\rm eff}$+m_ν model.

	P18	P18 + BAO	P18 + BAO + R19
$\omega_{\rm b}$	0.02217 ± 0.00022	0.02222 ± 0.00020	0.02257 ± 0.00018
$\omega_{\rm c}$	0.1158 ± 0.0034	0.1158 ± 0.0032	0.1212 ± 0.0031
H_0 [km s^{-1}Mpc^{-1}]	66.7 ± 1.8 (3.2σ)	$67.2 \pm 1.1 (3.8\sigma)$	69.96 ± 0.93 (2.1σ)
τ	$0.0554^{+0.0064}_{-0.0076}$	$0.0556^{+0.0063}_{-0.0075}$	$0.0577^{+0.0069}_{-0.0082}$
$\ln\left(10^{10}A_{\rm s}\right)$	3.039 ± 0.017	3.039 ± 0.016	3.057 ± 0.016
$n_{\rm s}$	0.9582 ± 0.0084	0.9596 ± 0.0074	0.9745 ± 0.0064
N_{pl} [M$_{\rm pl}$]	< 1.000050 (95% CL)	< 1.000042 (95% CL)	< 1.000040 (95% CL)
m_ν [eV]	< 0.26 (95% CL)	< 0.17 (95% CL)	< 0.14 (95% CL)
$N_{\rm eff}$	2.73 ± 0.21	2.75 ± 0.21	3.14 ± 0.20
γ_{PN}	> 0.999950 (95% CL)	> 0.9958 (95% CL)	> 0.9960 (95% CL)
β_{PN}	< 1.0000041 (95% CL)	< 1.0000035 (95% CL)	< 1.0000033 (95% CL)
$\delta G_{\rm N}/G_{\rm N}$ (z=0)	> -0.046 (95% CL)	> -0.040 (95% CL)	> -0.037 (95% CL)
$10^{13}\dot{G}_{\rm N}/G_{\rm N}$ (z=0) [yr^{-1}]	$> -6.7 \times 10^{-9}$ (95% CL)	$> -5.7 \times 10^{-9}$ (95% CL)	$> -5.5 \times 10^{-9}$ (95% CL)
$G_{\rm N}/G$ (z=0)	> 0.999975 (95% CL)	> 0.999979 (95% CL)	> 0.999980 (95% CL)
$\Omega_{\rm m}$	$0.310^{+0.016}_{-0.018}$	0.3056 ± 0.0074	0.2939 ± 0.0064
σ_8	$0.808^{+0.024}_{-0.015}$	$0.814^{+0.015}_{-0.011}$	0.833 ± 0.012
r_s [Mpc]	$149.3^{+1.8}_{-2.1}$	149.2 ± 1.9	145.4 ± 1.7
$\Delta\chi^2$	3.0	0.4	−0.6

Table 8. Constraints on main and derived parameters (at 68% CL if not otherwise stated) considering P18 in combination with BAO and BAO + R19 for the CC+$N_{\rm eff}$+m_ν model.

References

[1] A. G. Riess *et al.*, Astrophys. J. **826** (2016) no.1, 56 doi:10.3847/0004-637X/826/1/56 [arXiv:1604.01424 [astro-ph.CO]].

[2] A. G. Riess *et al.*, Astrophys. J. **861** (2018) no.2, 126 doi:10.3847/1538-4357/aac82e [arXiv:1804.10655 [astro-ph.CO]].

[3] V. Bonvin *et al.*, Mon. Not. Roy. Astron. Soc. **465** (2017) no.4, 4914 doi:10.1093/mnras/stw3006 [arXiv:1607.01790 [astro-ph.CO]].

[4] S. Birrer *et al.*, Mon. Not. Roy. Astron. Soc. **484** (2019) 4726 doi:10.1093/mnras/stz200 [arXiv:1809.01274 [astro-ph.CO]].

[5] K. C. Wong *et al.*, arXiv:1907.04869 [astro-ph.CO].

[6] P. A. R. Ade *et al.* [Planck Collaboration], Astron. Astrophys. **594** (2016) A13 doi:10.1051/0004-6361/201525830 [arXiv:1502.01589 [astro-ph.CO]].

[7] N. Aghanim *et al.* [Planck Collaboration], arXiv:1807.06209 [astro-ph.CO].

[8] A. G. Riess, S. Casertano, W. Yuan, L. M. Macri and D. Scolnic, Astrophys. J. **876** (2019) no.1, 85 doi:10.3847/1538-4357/ab1422 [arXiv:1903.07603 [astro-ph.CO]].

[9] A. G. Riess *et al.*, Astrophys. J. **855** (2018) no.2, 136 doi:10.3847/1538-4357/aaadb7 [arXiv:1801.01120 [astro-ph.SR]].

[10] G. E. Addison, Y. Huang, D. J. Watts, C. L. Bennett, M. Halpern, G. Hinshaw and J. L. Weiland, Astrophys. J. **818** (2016) no.2, 132 doi:10.3847/0004-637X/818/2/132 [arXiv:1511.00055 [astro-ph.CO]].

[11] N. Aghanim *et al.* [Planck Collaboration], Astron. Astrophys. **607** (2017) A95 doi:10.1051/0004-6361/201629504 [arXiv:1608.02487 [astro-ph.CO]].

[12] K. Aylor, M. Joy, L. Knox, M. Millea, S. Raghunathan and W. L. K. Wu, Astrophys. J. **874** (2019) no.1, 4 doi:10.3847/1538-4357/ab0898 [arXiv:1811.00537 [astro-ph.CO]].

[13] G. Efstathiou, Mon. Not. Roy. Astron. Soc. **440** (2014) no.2, 1138 doi:10.1093/mnras/stu278 [arXiv:1311.3461 [astro-ph.CO]].

[14] M. Rigault *et al.*, Astrophys. J. **802** (2015) no.1, 20 doi:10.1088/0004-637X/802/1/20 [arXiv:1412.6501 [astro-ph.CO]].

[15] M. Rigault *et al.* [Nearby Supernova Factory Collaboration], arXiv:1806.03849 [astro-ph.CO].

[16] W. L. Freedman *et al.*, doi:10.3847/1538-4357/ab2f73 arXiv:1907.05922 [astro-ph.CO].

[17] D. O. Jones *et al.*, Astrophys. J. **867** (2018) no.2, 108 doi:10.3847/1538-4357/aae2b9 [arXiv:1805.05911 [astro-ph.CO]].

[18] B. M. Rose, P. M. Garnavich and M. A. Berg, Astrophys. J. **874** (2019) no.1, 32 doi:10.3847/1538-4357/ab0704 [arXiv:1902.01433 [astro-ph.CO]].

[19] W. Yuan, A. G. Riess, L. M. Macri, S. Casertano and D. Scolnic, Astrophys. J. **886** (2019) 61 doi:10.3847/1538-4357/ab4bc9 [arXiv:1908.00993 [astro-ph.GA]].

[20] S. Dhawan, D. Brout, D. Scolnic, A. Goobar, A. Riess and V. Miranda, [arXiv:2001.09260 [astro-ph.CO]].

[21] W. L. Freedman *et al.*, doi:10.3847/1538-4357/ab7339 arXiv:2002.01550 [astro-ph.GA].

[22] E. Mörtsell and S. Dhawan, JCAP **09** (2018), 025 doi:10.1088/1475-7516/2018/09/025 [arXiv:1801.07260 [astro-ph.CO]].

[23] L. Knox and M. Millea, Phys. Rev. D **101** (2020) no.4, 043533 doi:10.1103/PhysRevD.101.043533 [arXiv:1908.03663 [astro-ph.CO]].

[24] E. Di Valentino, A. Melchiorri and J. Silk, Phys. Lett. B **761** (2016) 242 doi:10.1016/j.physletb.2016.08.043 [arXiv:1606.00634 [astro-ph.CO]].

[25] E. Di Valentino, A. Melchiorri, E. V. Linder and J. Silk, Phys. Rev. D **96** (2017) no.2, 023523 doi:10.1103/PhysRevD.96.023523 [arXiv:1704.00762 [astro-ph.CO]].

[26] S. Vagnozzi, [arXiv:1907.07569 [astro-ph.CO]].

[27] E. Di Valentino, E. V. Linder and A. Melchiorri, Phys. Rev. D **97** (2018) no.4, 043528 doi:10.1103/PhysRevD.97.043528 [arXiv:1710.02153 [astro-ph.CO]].

[28] N. Khosravi, S. Baghram, N. Afshordi and N. Altamirano, Phys. Rev. D **99** (2019) no.10, 103526 doi:10.1103/PhysRevD.99.103526 [arXiv:1710.09366 [astro-ph.CO]].

[29] A. Banihashemi, N. Khosravi and A. H. Shirazi, Phys. Rev. D **99** (2019) no.8, 083509 doi:10.1103/PhysRevD.99.083509 [arXiv:1810.11007 [astro-ph.CO]].

[30] A. Banihashemi, N. Khosravi and A. H. Shirazi, arXiv:1808.02472 [astro-ph.CO].

[31] G. Benevento, W. Hu and M. Raveri, arXiv:2002.11707 [astro-ph.CO].

[32] S. Kumar and R. C. Nunes, Phys. Rev. D **94** (2016) no.12, 123511 doi:10.1103/PhysRevD.94.123511 [arXiv:1608.02454 [astro-ph.CO]].

[33] E. Di Valentino, A. Melchiorri and O. Mena, Phys. Rev. D **96** (2017) no.4, 043503 doi:10.1103/PhysRevD.96.043503 [arXiv:1704.08342 [astro-ph.CO]].

[34] W. Yang, S. Pan, E. Di Valentino, R. C. Nunes, S. Vagnozzi and D. F. Mota, JCAP **09** (2018), 019 doi:10.1088/1475-7516/2018/09/019 [arXiv:1805.08252 [astro-ph.CO]].

[35] E. Di Valentino, A. Melchiorri, O. Mena and S. Vagnozzi, Phys. Rev. D **101** (2020) no.6, 063502 doi:10.1103/PhysRevD.101.063502 [arXiv:1910.09853 [astro-ph.CO]].

[36] A. Gómez-Valent, V. Pettorino and L. Amendola, [arXiv:2004.00610 [astro-ph.CO]].

[37] H. Miao and Z. Huang, Astrophys. J. **868** (2018) no.1, 20 doi:10.3847/1538-4357/aae523 [arXiv:1803.07320 [astro-ph.CO]].

[38] G. E. Addison, D. J. Watts, C. L. Bennett, M. Halpern, G. Hinshaw and J. L. Weiland, Astrophys. J. **853** (2018) no.2, 119 doi:10.3847/1538-4357/aaa1ed [arXiv:1707.06547 [astro-ph.CO]].

[39] F. Beutler *et al.*, Mon. Not. Roy. Astron. Soc. **416** (2011) 3017 doi:10.1111/j.1365-2966.2011.19250.x [arXiv:1106.3366 [astro-ph.CO]].

[40] A. J. Ross, L. Samushia, C. Howlett, W. J. Percival, A. Burden and M. Manera, Mon. Not. Roy. Astron. Soc. **449** (2015) no.1, 835 doi:10.1093/mnras/stv154 [arXiv:1409.3242 [astro-ph.CO]].

[41] S. Alam *et al.* [BOSS Collaboration], Mon. Not. Roy. Astron. Soc. **470** (2017) no.3, 2617 doi:10.1093/mnras/stx721 [arXiv:1607.03155 [astro-ph.CO]].

[42] Y. Akrami *et al.* [Planck Collaboration], arXiv:1807.06205 [astro-ph.CO].

[43] J. L. Bernal, L. Verde and A. G. Riess, JCAP **1610** (2016) 019 doi:10.1088/1475-7516/2016/10/019 [arXiv:1607.05617 [astro-ph.CO]].

[44] F. Y. Cyr-Racine and K. Sigurdson, Phys. Rev. D **90** (2014) no.12, 123533 doi:10.1103/PhysRevD.90.123533 [arXiv:1306.1536 [astro-ph.CO]].

[45] L. Lancaster, F. Y. Cyr-Racine, L. Knox and Z. Pan, JCAP **1707** (2017) 033 doi:10.1088/1475-7516/2017/07/033 [arXiv:1704.06657 [astro-ph.CO]].

[46] M. A. Buen-Abad, M. Schmaltz, J. Lesgourgues and T. Brinckmann, JCAP **1801** (2018) 008 doi:10.1088/1475-7516/2018/01/008 [arXiv:1708.09406 [astro-ph.CO]].

[47] E. Di Valentino, C. Bøehm, E. Hivon and F. R. Bouchet, Phys. Rev. D **97** (2018) no.4, 043513 doi:10.1103/PhysRevD.97.043513 [arXiv:1710.02559 [astro-ph.CO]].

[48] F. D'Eramo, R. Z. Ferreira, A. Notari and J. L. Bernal, JCAP **1811** (2018) 014 doi:10.1088/1475-7516/2018/11/014 [arXiv:1808.07430 [hep-ph]].

[49] V. Poulin, K. K. Boddy, S. Bird and M. Kamionkowski, Phys. Rev. D **97** (2018) no.12, 123504 doi:10.1103/PhysRevD.97.123504 [arXiv:1803.02474 [astro-ph.CO]].

[50] C. D. Kreisch, F. Y. Cyr-Racine and O. Doré, arXiv:1902.00534 [astro-ph.CO].

[51] N. Blinov, K. J. Kelly, G. Z. Krnjaic and S. D. McDermott, Phys. Rev. Lett. **123** (2019) no.19, 191102 doi:10.1103/PhysRevLett.123.191102 [arXiv:1905.02727 [astro-ph.CO]].

[52] V. Poulin, T. L. Smith, T. Karwal and M. Kamionkowski, Phys. Rev. Lett. **122** (2019) no.22, 221301 doi:10.1103/PhysRevLett.122.221301 [arXiv:1811.04083 [astro-ph.CO]].

[53] P. Agrawal, F. Y. Cyr-Racine, D. Pinner and L. Randall, arXiv:1904.01016 [astro-ph.CO].

[54] T. L. Smith, V. Poulin and M. A. Amin, Phys. Rev. D **101** (2020) no.6, 063523 doi:10.1103/PhysRevD.101.063523 [arXiv:1908.06995 [astro-ph.CO]].

[55] S. Alexander and E. McDonough, Phys. Lett. B **797** (2019), 134830 doi:10.1016/j.physletb.2019.134830 [arXiv:1904.08912 [astro-ph.CO]].

[56] M. X. Lin, G. Benevento, W. Hu and M. Raveri, Phys. Rev. D **100** (2019) no.6, 063542 doi:10.1103/PhysRevD.100.063542 [arXiv:1905.12618 [astro-ph.CO]].

[57] M. Braglia, W. T. Emond, F. Finelli, A. E. Gumrukcuoglu and K. Koyama, [arXiv:2005.14053 [astro-ph.CO]].

[58] D. K. Hazra, A. Shafieloo and T. Souradeep, JCAP **1904** (2019) 036 doi:10.1088/1475-7516/2019/04/036 [arXiv:1810.08101 [astro-ph.CO]].

[59] M. Liu and Z. Huang, arXiv:1910.05670 [astro-ph.CO].

[60] C. T. Chiang and A. Slosar, arXiv:1811.03624 [astro-ph.CO].

[61] M. Liu, Z. Huang, X. Luo, H. Miao, N. K. Singh and L. Huang, arXiv:1912.00190 [astro-ph.CO].

[62] C. Umiltà, M. Ballardini, F. Finelli and D. Paoletti, JCAP **1508** (2015) 017 doi:10.1088/1475-7516/2015/08/017 [arXiv:1507.00718 [astro-ph.CO]].

[63] M. Ballardini, F. Finelli, C. Umiltà and D. Paoletti, JCAP **1605** (2016) 067 doi:10.1088/1475-7516/2016/05/067 [arXiv:1601.03387 [astro-ph.CO]].

[64] R. C. Nunes, JCAP **1805** (2018) 052 doi:10.1088/1475-7516/2018/05/052 [arXiv:1802.02281 [gr-qc]].

[65] M. X. Lin, M. Raveri and W. Hu, Phys. Rev. D **99** (2019) no.4, 043514 doi:10.1103/PhysRevD.99.043514 [arXiv:1810.02333 [astro-ph.CO]].

[66] M. Rossi, M. Ballardini, M. Braglia, F. Finelli, D. Paoletti, A. A. Starobinsky and C. Umiltà, Phys. Rev. D **100** (2019) no.10, 103524 doi:10.1103/PhysRevD.100.103524 [arXiv:1906.10218 [astro-ph.CO]].

[67] J. Solà Peracaula, A. Gomez-Valent, J. de Cruz Pérez and C. Moreno-Pulido, Astrophys. J. **886** (2019) no.1, L6 doi:10.3847/2041-8213/ab53e9 [arXiv:1909.02554 [astro-ph.CO]].

[68] M. Zumalacárregui, arXiv:2003.06396 [astro-ph.CO].

[69] D. Wang and D. Mota, arXiv:2003.10095 [astro-ph.CO].

[70] G. Ballesteros, A. Notari and F. Rompineve, [arXiv:2004.05049 [astro-ph.CO]].

[71] M. Braglia, M. Ballardini, W. T. Emond, F. Finelli, A. E. Gümrükçüoğlu, K. Koyama and D. Paoletti, [arXiv:2004.11161 [astro-ph.CO]].

[72] H. Motohashi, A. A. Starobinsky and J. Yokoyama, Phys. Rev. Lett. **110** (2013) 121302, doi:10.1103/PhysRevLett.110.121302 [arXiv:1203.6828 [astro-ph.CO]].

[73] A. Chudaykin, D. Gorbunov, A. Starobinsky and R. Burenin, JCAP **05** (2015), 004 doi:10.1088/1475-7516/2015/05/004 [arXiv:1412.5239 [astro-ph.CO]].

[74] S. Vagnozzi, E. Giusarma, O. Mena, K. Freese, M. Gerbino, S. Ho and M. Lattanzi, Phys. Rev. D **96** (2017) no.12, 123503 doi:10.1103/PhysRevD.96.123503 [arXiv:1701.08172 [astro-ph.CO]].

[75] S. Roy Choudhury and S. Hannestad, arXiv:1907.12598 [astro-ph.CO].

[76] A. Barreira, B. Li, C. Baugh and S. Pascoli, Phys. Rev. D **90** (2014) no.2, 023528 doi:10.1103/PhysRevD.90.023528 [arXiv:1404.1365 [astro-ph.CO]].

[77] M. Tanabashi *et al.* [Particle Data Group], Phys. Rev. D **98** (2018) no.3, 030001 doi:10.1103/PhysRevD.98.030001

[78] P. Ade *et al.* [Simons Observatory Collaboration], JCAP **1902** (2019) 056 doi:10.1088/1475-7516/2019/02/056 [arXiv:1808.07445 [astro-ph.CO]].

[79] K. N. Abazajian *et al.* [CMB-S4 Collaboration], arXiv:1610.02743 [astro-ph.CO].

[80] M. Levi *et al.* [DESI Collaboration], arXiv:1308.0847 [astro-ph.CO].

[81] R. Laureijs *et al.* [EUCLID Collaboration], arXiv:1110.3193 [astro-ph.CO].

[82] L. Amendola *et al.* [Euclid Theory Working Group], Living Rev. Rel. **16** (2013) 6 doi:10.12942/lrr-2013-6 [arXiv:1206.1225 [astro-ph.CO]].

[83] P. A. Abell *et al.* [LSST Science and LSST Project Collaborations], arXiv:0912.0201 [astro-ph.IM].

[84] R. Maartens *et al.* [SKA Cosmology SWG Collaboration], PoS AASKA **14** (2015) 016 doi:10.22323/1.215.0016 [arXiv:1501.04076 [astro-ph.CO]].

[85] D. J. Bacon *et al.* [SKA Collaboration], [arXiv:1811.02743 [astro-ph.CO]].

[86] T. Brinckmann, D. C. Hooper, M. Archidiacono, J. Lesgourgues and T. Sprenger, JCAP **1901** (2019) 059 doi:10.1088/1475-7516/2019/01/059 [arXiv:1808.05955 [astro-ph.CO]].

[87] D. Alonso, E. Bellini, P. G. Ferreira and M. Zumalacárregui, Phys. Rev. D **95** (2017) no.6, 063502 doi:10.1103/PhysRevD.95.063502 [arXiv:1610.09290 [astro-ph.CO]].

[88] M. Ballardini, D. Sapone, C. Umiltà, F. Finelli and D. Paoletti, JCAP **1905** (2019) 049 doi:10.1088/1475-7516/2019/05/049 [arXiv:1902.01407 [astro-ph.CO]].

[89] N. Bellomo, E. Bellini, B. Hu, R. Jimenez, C. Pena-Garay and L. Verde, JCAP **1702** (2017) 043 doi:10.1088/1475-7516/2017/02/043 [arXiv:1612.02598 [astro-ph.CO]].

[90] P. Jordan, Nature **164** (1949) 637. doi:10.1038/164637a0

[91] C. Brans and R. H. Dicke, Phys. Rev. **124** (1961) 925. doi:10.1103/PhysRev.124.925

[92] X. l. Chen and M. Kamionkowski, Phys. Rev. D **60** (1999) 104036 doi:10.1103/PhysRevD.60.104036 [astro-ph/9905368].

[93] R. Nagata, T. Chiba and N. Sugiyama, Phys. Rev. D **69** (2004) 083512 doi:10.1103/PhysRevD.69.083512 [astro-ph/0311274].

[94] V. Acquaviva, C. Baccigalupi, S. M. Leach, A. R. Liddle and F. Perrotta, Phys. Rev. D **71** (2005) 104025 doi:10.1103/PhysRevD.71.104025 [astro-ph/0412052].

[95] A. Avilez and C. Skordis, Phys. Rev. Lett. **113** (2014) no.1, 011101 doi:10.1103/PhysRevLett.113.011101 [arXiv:1303.4330 [astro-ph.CO]].

[96] Y. C. Li, F. Q. Wu and X. Chen, Phys. Rev. D **88** (2013) 084053 doi:10.1103/PhysRevD.88.084053 [arXiv:1305.0055 [astro-ph.CO]].

[97] J. Ooba, K. Ichiki, T. Chiba and N. Sugiyama, Phys. Rev. D **93** (2016) no.12, 122002 doi:10.1103/PhysRevD.93.122002 [arXiv:1602.00809 [astro-ph.CO]].

[98] G. W. Horndeski, Int. J. Theor. Phys. **10** (1974) 363. doi:10.1007/BF01807638

[99] J. P. Uzan, Phys. Rev. D **59** (1999) 123510 doi:10.1103/PhysRevD.59.123510 [gr-qc/9903004].

[100] F. Perrotta, C. Baccigalupi and S. Matarrese, Phys. Rev. D **61** (1999) 023507 doi:10.1103/PhysRevD.61.023507 [astro-ph/9906066].

[101] N. Bartolo and M. Pietroni, Phys. Rev. D **61** (2000) 023518 doi:10.1103/PhysRevD.61.023518 [hep-ph/9908521].

[102] L. Amendola, Phys. Rev. D **60** (1999) 043501 doi:10.1103/PhysRevD.60.043501 [astro-ph/9904120].

[103] T. Chiba, Phys. Rev. D **60** (1999) 083508 doi:10.1103/PhysRevD.60.083508 [gr-qc/9903094].

[104] B. Boisseau, G. Esposito-Farese, D. Polarski and A. A. Starobinsky, Phys. Rev. Lett. **85** (2000) 2236, doi:10.1103/PhysRevLett.85.2236 [gr-qc/0001066].

[105] C. M. Will, Living Rev. Rel. **17** (2014) 4 doi:10.12942/lrr-2014-4 [arXiv:1403.7377 [gr-qc]].

[106] B. Bertotti, L. Iess and P. Tortora, Nature **425** (2003) 374. doi:10.1038/nature01997

[107] A. Y. Kamenshchik, E. Pozdeeva, A. Starobinsky, A. Tronconi, G. Venturi and S. Y. Vernov, Phys. Rev. D **97** (2018) no.2, 023536 doi:10.1103/PhysRevD.97.023536 [arXiv:1710.02681 [gr-qc]].

[108] B. Audren, J. Lesgourgues, K. Benabed and S. Prunet, JCAP **1302** (2013) 001, doi:10.1088/1475-7516/2013/02/001 [arXiv:1210.7183 [astro-ph.CO]].

[109] T. Brinckmann and J. Lesgourgues, Phys. Dark Univ. **24** (2019) 100260 doi:10.1016/j.dark.2018.100260 [arXiv:1804.07261 [astro-ph.CO]].

[110] J. Lesgourgues, arXiv:1104.2932 [astro-ph.IM].

[111] D. Blas, J. Lesgourgues and T. Tram, JCAP **1107** (2011) 034 doi:10.1088/1475-7516/2011/07/034 [arXiv:1104.2933 [astro-ph.CO]].

[112] A. Lewis, [arXiv:1910.13970 [astro-ph.IM]].

[113] D. Paoletti, M. Braglia, F. Finelli, M. Ballardini and C. Umiltà, Phys. Dark Univ. **25** (2019), 100307 doi:10.1016/j.dark.2019.100307 [arXiv:1809.03201 [astro-ph.CO]].

[114] N. Aghanim *et al.* [Planck Collaboration], arXiv:1907.12875 [astro-ph.CO].

[115] N. Aghanim *et al.* [Planck Collaboration], arXiv:1807.06210 [astro-ph.CO].

[116] A. J. Ross *et al.* [BOSS Collaboration], Mon. Not. Roy. Astron. Soc. **464** (2017) no.1, 1168 doi:10.1093/mnras/stw2372 [arXiv:1607.03145 [astro-ph.CO]].

[117] M. Vargas-Magaña *et al.*, Mon. Not. Roy. Astron. Soc. **477** (2018) no.1, 1153 doi:10.1093/mnras/sty571 [arXiv:1610.03506 [astro-ph.CO]].

[118] F. Beutler *et al.* [BOSS Collaboration], Mon. Not. Roy. Astron. Soc. **464** (2017) no.3, 3409 doi:10.1093/mnras/stw2373 [arXiv:1607.03149 [astro-ph.CO]].

[119] R. Adam *et al.* [Planck Collaboration], Astron. Astrophys. **594** (2016) A1 doi:10.1051/0004-6361/201527101 [arXiv:1502.01582 [astro-ph.CO]].

[120] N. Aghanim *et al.* [Planck Collaboration], Astron. Astrophys. **594** (2016) A11 doi:10.1051/0004-6361/201526926 [arXiv:1507.02704 [astro-ph.CO]].

[121] J. G. Williams, S. G. Turyshev and D. H. Boggs, Phys. Rev. Lett. **93** (2004), 261101 doi:10.1103/PhysRevLett.93.261101 [arXiv:gr-qc/0411113 [gr-qc]].

[122] L. Anderson *et al.* [BOSS Collaboration], Mon. Not. Roy. Astron. Soc. **441** (2014) no.1, 24 doi:10.1093/mnras/stu523 [arXiv:1312.4877 [astro-ph.CO]].

[123] S. Hannestad, Ann. Rev. Nucl. Part. Sci. **56** (2006) 137 doi:10.1146/annurev.nucl.56.080805.140548 [hep-ph/0602058].

[124] J. Lesgourgues, G. Mangano, G. Miele and S. Pastor, (2013).

[125] S. Dodelson and M. S. Turner, Phys. Rev. D **46** (1992) 3372. doi:10.1103/PhysRevD.46.3372

[126] B. D. Fields, S. Dodelson and M. S. Turner, Phys. Rev. D **47** (1993) 4309 doi:10.1103/PhysRevD.47.4309 [astro-ph/9210007].

[127] A. D. Dolgov and M. Fukugita, Phys. Rev. D **46** (1992) 5378. doi:10.1103/PhysRevD.46.5378

[128] G. Mangano, G. Miele, S. Pastor, T. Pinto, O. Pisanti and P. D. Serpico, Nucl. Phys. B **729** (2005) 221 doi:10.1016/j.nuclphysb.2005.09.041 [hep-ph/0506164].

[129] S. Bashinsky and U. Seljak, Phys. Rev. D **69** (2004) 083002 doi:10.1103/PhysRevD.69.083002 [astro-ph/0310198].

[130] S. Hannestad, Phys. Rev. Lett. **95** (2005) 221301 doi:10.1103/PhysRevLett.95.221301 [astro-ph/0505551].

[131] J. Lesgourgues and S. Pastor, Phys. Rept. **429** (2006) 307 doi:10.1016/j.physrep.2006.04.001 [astro-ph/0603494].

[132] Y. Y. Y. Wong, Ann. Rev. Nucl. Part. Sci. **61** (2011) 69 doi:10.1146/annurev-nucl-102010-130252 [arXiv:1111.1436 [astro-ph.CO]].

[133] M. Archidiacono, T. Brinckmann, J. Lesgourgues and V. Poulin, JCAP **1702** (2017) 052 doi:10.1088/1475-7516/2017/02/052 [arXiv:1610.09852 [astro-ph.CO]].

[134] C. Cartis, J. Fiala, B. Marteau and L. Roberts, 2018. [arXiv:1804.00154 [math.OC]].

[135] C. Cartis, L. Roberts and O. Sheridan-Methven, 2018. [arXiv:1812.11343 [math.OC]].

[136] M.J.D. Powell, "The BOBYQA Algorithm for Bound Constrained Optimization without Derivatives", (Technical Report 2009/NA06, DAMTP, University of Cambridge).

[137] J. Torrado and A. Lewis, [arXiv:2005.05290 [astro-ph.IM]].

[138] F. Cooper and G. Venturi, Phys. Rev. D **24** (1981) 3338. doi:10.1103/PhysRevD.24.3338

[139] C. Wetterich, Nucl. Phys. B **302** (1988) 645. doi:10.1016/0550-3213(88)90192-7

[140] F. Finelli, A. Tronconi and G. Venturi, Phys. Lett. B **659** (2008), 466-470 doi:10.1016/j.physletb.2007.11.053 [arXiv:0710.2741 [astro-ph]].